MOLECULAR PHYSICS, 1996, VOL. 89, NO. 2, 373–401

Intramolecular coupling between non-penetrating high molecular Rydberg states

By M. BIXON and JOSHUA JORTNER
School of Chemistry, Tel Aviv University, Ramat Aviv, 69978 Tel Aviv, Israel

(*Received 8 February 1996; accepted 26 March 1996*)

We address a central question in the realm of the dynamics of high-n (= 40–250) Rydberg states of diatomics and large molecules. What is the coupling responsible for the 'global' l mixing, which results in the breakdown of the n^3 scaling law for the non-radiative lifetimes and for the lifetime lengthening (by two to four orders of magnitude) of these states? To explore the implications of intramolecular interactions on l mixing and on electronic–rotational energy exchange we analysed the intramolecular couplings of the ion core dipole, quadrupole and (anisotropic) polarizability with a non-penetrating ($l \geqslant 3$) Rydberg electron, in conjunction with the energy gaps between proximal pairs of energy levels. Calculations of the energy gaps and the couplings were performed for the high-n non-penetrating Rydberg states of NO and for model 'light' (B = 19 cm^{-1}) and 'heavy' (B = 0·05 cm^{-1}) polar molecules. All the intramolecular interactions are of the form of a power law proportional to $l^{-\eta}$, with η being determined by the nature of the long-range coupling, by the l dependence of the quantum defects for multipole couplings and by the l dependence of angular integrals. We established a bottleneck effect for the intramolecular couplings between non-penetrating ($l \geqslant 3$) states. For n- and N^+-changing dipole, quadrupole and polarizability interactions the energetics of the proximal pairs of levels, in conjunction with the bottleneck effect, prohibit the $|n, l, N^+, N\rangle - |n', l', N^{+\prime}, N\rangle$, l ($\geqslant 3$) couplings (with $n \neq n'$) and the electronic–rotational energy exchange. For n- and N^+-conserving quadrupole and polarizability interactions, the l ($\geqslant 3$) mixing (which prevails only for $l \leqslant N^+ + N$) is also prohibited by the bottleneck effect. 'Global' intramolecular l mixing (with both $n \neq n'$ and $n = n'$) in diatomics and in large molecules is precluded, implying that the dramatic lengthening of the non-radiative lifetimes of high-n Rydberg states can be induced only by exterior electric field coupling.

1. Introduction

Recent experimental [1–14] and theoretical [15–30] studies focused on the spectroscopy and dynamics of high-n (= 40–250) Rydberg states of diatomic and polyatomic molecules, which were interrogated by time-resolved zero-electron-kinetic-energy (ZEKE) spectroscopy [1–7, 12–14] and by time-resolved pulsed field ionization (PFI) ion-counting spectroscopy [8, 9]. A major issue regarding the understanding of radiationless transitions of high-n molecular Rydberg states, which involve pre-dissociation and autoionization for diatomics and for polyatomics and/or internal conversion for large molecules, pertains to the spectroscopic and dynamic manifestations of the intramolecular coupling. The traditional description of high-n Rydberg states rests on the notion of weak coupling between the angular momentum of the Rydberg electron and the ion core rotation, that is the Hund coupling case (d) [31], while perturbations due to (off-diagonal) intramolecular couplings will exhibit deviations from this coupling scheme, resulting in electronic–rotational energy

0026–8976/96 $12·00

exchange and/or mixing of states of different n [27–33]. This intramolecular coupling involves long-range Rydberg electron–core multiple and polarizability interactions, for example Rydberg electron–core dipole and quadrupole coupling [27–30, 34] for a polar molecule (HCl [29], NO [26] and H_2O [30]), or Rydberg electron–core quadrupole coupling [27–30, 34] for a homonuclear diatomic molecule (H_2 [27, 28] and N_2 [14]). Regarding the spectroscopic manifestations of intramolecular coupling between bound Rydberg states, the anomalous (type A) transitions in the ZEKE spectrum of H_2O [35] were explained by Gilbert and Child [30] and by Lee *et al.* [36] in terms of the intramolecular Rydberg electron–core dipole interaction, which mixes an nd ($n \approx 50$) state (from a sparse electronic manifold) with a dense n'p ($n' \approx 330$) electronic manifold. Of considerable interest is the dynamics of high-n Rydberg states [1–14], which exhibits the breakdown of the n^3 scaling law [31, 37–43] and a dramatic (two to four orders of magnitude) lengthening of non-radiative lifetimes (the dilution effect). Even and co-workers [7, 18–21] have proposed that high-n Rydberg dynamics are dominated by the intramolecular coupling between the Rydberg electron and the rotating core dipole, which results in 'down' ('up') relaxation to lower (higher) Rydberg states. Furthermore, Rabani *et al.* [20, 21] suggested that weak electric fields reduce the frequency of the close encounter of the Rydberg electron with the core, resulting in the retardation of the electronic–rotational energy exchange. Alternatively, the dynamics of high Rydberg states was accounted for by the l (or lm_l) coupling and mixing model [8, 9, 15–17, 22–26] induced by a weak electric field ($F \approx 0{\cdot}05$–$0{\cdot}1$ V cm^{-1}) inevitably present in the system. This model was advanced by Bordas *et al.* [15] and by Chupka [16, 17] and elaborated on by Merkt and Zare [22], Jortner and Bixon [23], Bixon and Jortner [24–26] and Vrakking and Lee [8, 9]. The field-induced coupling and mixing model provides a semiquantitative description for the autoionization dynamics of the $^2P_{1/2}np'[3/2]_1$ (n = 100–280) Rydberg states of Ar [13, 25] and for the pre-dissociation dynamics of the nf ($N^+ = 2$) (n = 40–95) and np ($N^+ = 0$) (n = 70–125) Rydberg series of NO [8, 9, 26]. Both atomic autoionization [13, 25] and molecular pre-dissociation [8, 9, 26] exhibit a marked lifetime lengthening, which is manifested at $n \geqslant 110$ for the autoionizing np' series of Ar [13, 25] and at $n > 65$ and $n > 116$ for the pre-dissociation of the f series and of the p series respectively of NO [8, 9, 26]. For atomic autoionization the electric field l [15–17, 23–26] (or lm_l) [22] mixing is exclusive. As far as molecular Rydberg states are concerned, both intramolecular Rydberg electron–core coupling and exterior electric field coupling mechanisms may prevail simultaneously.

In this paper we analyse the dynamic implications of intramolecular coupling of high-n Rydberg states. Non-penetrating ($l \geqslant 3$) high-n molecular Rydberg states interact with the molecular ion core via its multipole moments and polarizability [26–30, 34]. The question that we address in this paper is whether intramolecular Rydberg electron–core coupling can exhibit a 'global' l mixing (i.e. the mixing of all the $l = 0$---$(n-1)$ states corresponding to an n given value, or to a set of n values) and/or electronic–rotational energy exchange, which will result in the breakdown of the n^3 scaling law for the lifetimes of high-n Rydberg states in a field-free molecule. On the basis of an analysis of the non-penetrating high-n Rydberg level structure and intramolecular Rydberg electron–core dipole, quadrupole and anisotropic polarizability couplings of model molecular systems we shall demonstrate that intramolecular Rydberg electron–core couplings firstly do not induce l ($\geqslant 3$) mixing (with $n \neq n'$) between different core rotational angular momentum states N^+, prohibiting electronic–rotational energy exchange between states of different n, and

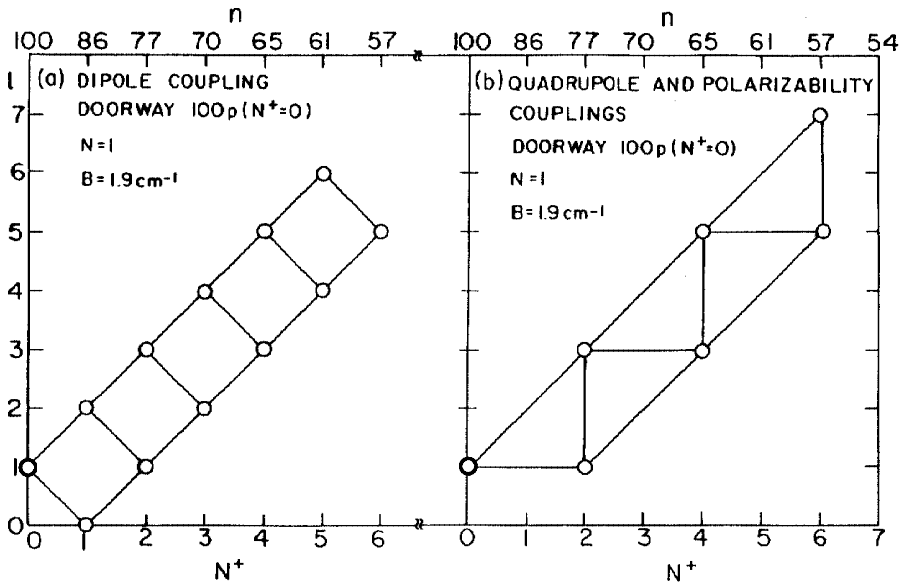

Figure 1. A branching diagram in the l, N^+ plane (at fixed N) for (*a*) intramolecular dipole coupling and (*b*) quadrupole and polarizability coupling. The open circles (○) represent the states accessible via coupling to the 100p ($N^+ = 0$, $N = 1$) doorway state (⊙). The total angular momentum is $N = 1$. The lines represent intramolecular couplings between proximal pairs of states subjected to the appropriate selection rules. The n upper scale represents the n values for proximal pairs of states for a model molecule with $B = 1{\cdot}9\ \mathrm{cm}^{-1}$.

secondly do not result in l ($\geqslant 3$) mixing within a single n manifold between N^+-conserving states. From our analysis of the implication of intramolecular interactions we conclude that 'global' l mixing cannot result from intramolecular coupling and can be induced only by exterior electric field coupling [8, 9, 15–17, 22–26]. The ineffectiveness of intramolecular 'global' l mixing in the context of the dramatic lifetime lengthening of high-n Rydberg states, which is considered herein, bears a close analogy to a previous analysis [44–46] of rotational autoionization accompanied by large core rotational angular momentum exchange in diatomics. This rotational autoionization is mediated by the coupling between discrete states. In this context Bordas *et al.* [44] pointed out that non-penetrating high-l Rydberg states are ineffective in electronic–rotational energy exchange, while Mahon *et al.* [45] and Merkt *et al.* [46] have shown that a series of sequential intramolecular multipole interactions via virtual mediating states are ineffective. Accordingly, mediated rotational autoionization is induced by exterior electric-field-induced coupling [44–46].

2. Level structure and intramolecular interactions

We first specify the field-free level structure for high-n Rydberg manifold(s) of a diatomic molecule, which serves as a generic example for the intramolecular Rydberg coupling and dynamics. We shall limit ourselves to a single vibrational state $v = 0$ of the molecular ion core. As n increases, the angular momentum $\mathbf{l}$ of the Rydberg electron becomes weakly coupled to the rotational angular momentum $\mathbf{N}^+$ of the

molecular core, whereupon the system is reasonably well described by the Hund coupling case (d). The angular momentum (excluding the spin) is $\mathbf{N} = \mathbf{l} + \mathbf{N}^+$, with a projection M_N, forming the total angular momentum $\mathbf{J} = \mathbf{N} + \mathbf{S}$, where $\mathbf{S}$ is the spin angular momentum. The Rydberg electron–core rotational states $|\kappa\rangle$ of a definite N are

$$|\kappa\rangle = |n, l, N^+, N, M_N\rangle, \tag{1}$$

with the energies $E(\kappa)$ being given by

$$E(\kappa) = IP(N^+) - \frac{\mathrm{Ryd}}{[n - \delta(l, \hat{\alpha})]^2}, \tag{2}$$

where Ryd is the Rydberg constant, $\delta(l, \hat{\alpha})$ is the quantum defect which depends on l and also on other quantum numbers $\hat{\alpha}$. $IP(N^+)$ is the ionization potential corresponding to the N^+ rotational state of the diatomic ion core, which is given by

$$IP(N^+) = IP(0) + BN^+(N^+ + 1), \tag{3}$$

where B is the rotational constant of the positive ion core and $IP(0)$ is the lowest ionization potential corresponding to $N^+ = 0$.

Disregarding the effects of line broadening and level shifts due to the decay channels for intramolecular radiationless decay, the field-free ($F = 0$) Hamiltonian of the diatomic molecule is

$$\mathbf{H} = \mathbf{H}_0 + \mathbf{H}_{\mathrm{int}}, \tag{4}$$

where the zero-order Hamiltonian $\mathbf{H}_0$ for the Hund coupling case (d) is

$$\mathbf{H}_0 = \sum_{\kappa} |\kappa\rangle E_\kappa \langle\kappa|, \tag{5}$$

being expressed in terms of equations (1) and (2). For non-penetrating ($l \geqslant 3$) Rydbergs $\mathbf{H}_{\mathrm{int}}$ is the intramolecular long-range interaction Hamiltonian [27, 28]

$$\mathbf{H}_{\mathrm{int}} = \tfrac{1}{2} \sum_{\kappa \neq \kappa'} \sum |\kappa\rangle\langle\kappa| H_{\mathrm{dipole}} + H_{\mathrm{quad}} + H_{\mathrm{pol}} |\kappa'\rangle\langle\kappa'|, \tag{6}$$

where H_{dipole} is the Rydberg electron–core (permanent) dipole interaction, H_{quad} is the Rydberg electron–core quadrupole interaction, while H_{pol} is the Rydberg electron–core polarizability interaction. $\mathbf{H}_{\mathrm{int}}$ induces deviations from the Hund coupling limit (d), which can be treated in a systematic manner. For a polar ionic core the intramolecular interaction is often (but not exclusively) dominated by H_{dipole}, which we shall now consider. The matrix elements for the Rydberg electron–core dipole coupling are [28]

$$\langle n, l, N^+, N, M_N | H_{\mathrm{dipole}} | n', l', N^{+\prime}, N', M'_N \rangle = -e\mu \langle nl | r^{-2} | n'l' \rangle f(l, N^+, N, M_N; l', N^{+\prime}, N', M'_N), \tag{7}$$

where μ is the dipole moment of the ion core, while $f(l, N^+, N, N_M; l', N^{+\prime}, N', M'_N)$ is

the angular integral. The matrix elements for the Rydberg electron–core quadrupole coupling are [27, 28]

$$\langle n, l, N^+, N, M \,|H_{\text{quad}}|\, n', l', N^{+\prime}, N', M'_N\rangle = -eQ\langle nl\,|r^{-3}|\,n'l'\rangle\, g(l, N^+, N, M_N; l', N^{+\prime}, N', M'_N), \quad (8)$$

where Q is the ionic core quadrupole moment and $g(l, N^+, N, M_N; l', N^{+\prime}, M'_N)$ is an angular integral. Finally, the matrix elements for the core polarizability interactions are [27, 28]

$$\langle n, l, N^+, N, M_N|H_{\text{pol}}|\, n', l', N^{+\prime}, N', M'_N\rangle = -e^2\langle n, l\,|r^{-4}|\,n', l'\rangle\left(\frac{\alpha}{2}\delta_{l,l'}\delta_{N^+,N^{+\prime}} + \frac{\gamma}{3}g(l, N^+, N, M_N; l', N^{+\prime}, N', M'_N)\right), \quad (9)$$

where $\alpha = (2\alpha_\perp + \alpha_\parallel)/3$ is the isotropic core polarizability, $\gamma = (\alpha_\perp - \alpha_\parallel)$ is the anisotropic core polarizability and $g(\cdot)$ is the angular integral.

The angular matrix elements $f(l, N^+, N, M_N; l', N^{+\prime}, N', M'_N)$ and $g(l, N^+, N, M_N; l', N^{+\prime}, N', M'_N)$ in equations (7)–(9) are of the form

$$\langle l, N^+, N, M_N|P_k(\cos\chi)|\, l', N^{+\prime}, N', M'_N\rangle = (-1)^{l+l'+N}\begin{Bmatrix} N' & N^+ & l \\ k & l' & N^{+\prime}\end{Bmatrix} \otimes \delta_{N,N'}\delta_{M_N M'_N}[(2l+1)(2l'+1)]^{1/2}\begin{bmatrix} l & k & l' \\ 0 & 0 & 0\end{bmatrix} \otimes [(2N^+ + 1)(2N^{+\prime}+1)]^{1/2}\begin{bmatrix} N^+ & k & N^{+\prime} \\ 0 & 0 & 0\end{bmatrix}, \quad (10)$$

where $k = 1$ for the dipole coupling angular integrals $f(\cdot)$ and $k = 2$ for the quadrupole and core polarization angular integrals $g(\cdot)$. The selection rules for the dipole coupling are

$$\Delta l = \pm 1, \quad \Delta N^+ = \pm 1, \quad \Delta N = 0, \quad \Delta M_N = 0. \quad (11)$$

The selection rules for the quadrupole coupling are

$$\Delta l = 0, \pm 2, \quad \Delta N^+ = 0, \pm 2, \quad \Delta N = 0. \quad (12)$$

The diagonal integral (8) for $\Delta l = \Delta N^+ = \Delta N = 0$ contributes to the quantum defect, while the off-diagonal integrals (with $\Delta N = 0$) contribute to the intramolecular interaction. The selection rules for the isotropic polarizability in equation (9) are $\Delta l = 0$, $\Delta N^+ = 0$, $\Delta N = 0$. The isotropic polarizability has only diagonal elements, which contribute to the quantum defect [27, 47–50]. For the anisotropic polarizability the selection rules are given by equation (12). The anisotropic polarizability contributes to the intramolecular interaction. Regarding the Rydberg electron–core polarizability coupling (equation (9)), it is worthwhile to point out that this representation implies an adiabatic separation between the motion of the slow Rydberg electron and the fast core electrons, that is an electronic Born–Oppenheimer separation, which was advanced by Bethe and Salpeter [37] for the Rydberg states of the He atom.

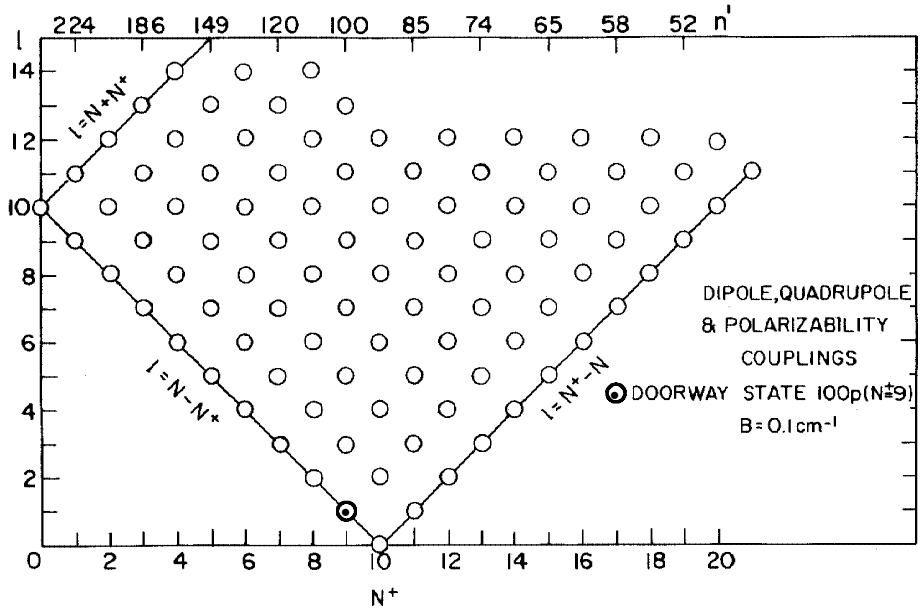

Figure 2. A branching diagram for the intramolecular dipole, quadrupole and polarizability couplings. The open circles (○) represent the states accessible via coupling to the 100p ($N_l^+ = 9$, $N = 10$) doorway state (⊙). The solid straight lines represent the limits of l subjected to angular momentum conservation. The n upper scale represents the n values for proximal pairs of states for a model molecule with $B = 0{\cdot}1\ \mathrm{cm}^{-1}$.

Buckingham [50] pioneered the analysis of long-range interaction for the quantum defects in the Hund coupling case (b). The off-diagonal matrix elements of H_{dipole} (equation (7)), H_{quad} (equation (8)) and H_{pol} (equation (9)) constitute the contributions to the (long-range) intramolecular interactions for non-penetrating Rydberg states for the Hund coupling case (d). The diagonal matrix elements of the H_{dipole} interactions vanish, while the diagonal matrix elements of H_{quad} and of H_{pol} provide the long-range contribution to the quantum defects [27, 47, 48]. The level structure in the unperturbed Hund coupling case (d) consists of 'l complexes' at each value of the core rotation quantum number N^+ with $(2l+1)$ degenerate sublevels with different values of N (for $N^+ > l$). The intramolecular dipole, quadrupole and anisotropic polarizability couplings between $|n, l, N^+, N\rangle$ and $|n', l', N^{+\prime}, N'\rangle$ states occur between members of 'l complexes' subjected to the appropriate selection rules, with N being conserved in all cases. In figure 1 we present a typical example for the schemes of the intramolecular couplings from the np ($N^+ = 0$, $N = 1$) doorway state ($n = 100$), which were experimentally studied [8, 9] for the Rydberg states of NO ($n = 70$–125). The intramolecular couplings which change the value of l, that is $\Delta l = \pm 1$ for H_{dipole} and $\Delta l = \pm 2$ for H_{quad} and H_{pol} are represented by non-horizontal lines in figure 1. The l-conserving couplings, that is, $\Delta l = 0$ ($0 \leftarrow\!/\!\rightarrow 0$ with $\Delta N^+ = \pm 2$) for H_{quad} and H_{pol} are represented by horizontal lines in figure 1(b). Of course, combinations of dipole ($\Delta l = \pm 1$) and of quadrupole and polarizability ($\Delta l = \pm 2, 0$) interactions are possible. The points in figures 1(a) and (b) span the grid of states which are accessible from the 100p ($N^+ = 0$, $N = 1$) doorway state and represent a narrow ladder in the range of l values $|N^+ - 1| \leqslant l \leqslant N^+ + 1$. With a larger value of N, which characterizes the doorway state, the ladder of accessible states becomes broader. Figure 2 presents a

typical example of a grid of states accessible by intramolecular couplings from the 100p ($N^+ = 9$, $N = 10$) doorway state. The accessible states via dipole ($\Delta l = \pm 1$), and via quadrupole and polarizability couplings ($\Delta l = \pm 2$), are restricted by the angular momentum conservation

$$|N^+ - N| \leqslant l \leqslant (N + N^+). \tag{13}$$

Two general types of intramolecular interaction, which are determined by the N^+ selection rules and by energy constraints on n (figures 1 and 2), can be distinguished.

(I) *n- and N^+-changing interactions*. These involve $|n, l, N^+, N\rangle - |n', l', N^{+\prime}, N\rangle$ pair couplings with a change in N^+, that is dipole couplings ($\Delta N^+ = \pm 1$) and quadrupole and anisotropic polarizability couplings ($\Delta N^+ = \pm 2$). $n'(\neq n)$ is chosen for the realization of a minimal energy gap between the proximal pair of states. The couplings are represented by pairs of points lying on non-horizontal ($\Delta l = \pm 1, \pm 2$) and horizontal ($\Delta l = 0$) lines in figure 2. The changes in n for the typical case are indicated in figure 1. The n- and N^+-changing dipole coupling, quadrupole and anisotropic polarizability couplings (with $\Delta l = \pm 2$) can induce direct l mixing (with $n \neq n'$), which corresponds to electronic–rotational Rydberg electron–core energy exchange.

(II) *n- and N^+-conserving interactions*. These correspond to $|n, l, N^+, N\rangle - |n, l \pm 2, N^+, N\rangle$ pairs of states with $\Delta N^+ = 0$, which conserve N^+, involving quadrupole and anisotropic polarizability ($\Delta l = \pm 2$) interactions. These couplings are indicated by vertical lines in figure 1(*b*) and correspond to neighbouring points lying on vertical lines in figure 2. Dipole coupling is precluded in this class by its selection rules (equation (11)). Ascending the l values for a fixed (initial) value of N^+ there is a cut-off at the upper limit for the accessible values of $l \leqslant (N + N^+)$ (equation (13)).

To provide an analysis of the intramolecular couplings, we require the radial integrals for the multipole and polarizability couplings (section 3 and appendix). Subsequently, input data (section 4) will be utilized for the analysis of n- and N^+-changing dipole, quadrupole and polarizability interactions (section 5) and of n- and N^+-conserving quadrupole and polarizability interactions (section 6) for the NO molecule and for model systems.

3. Radial integrals for intramolecular coupling between high-n Rydberg states

The intermolecular coupling terms of H_{dipole} (equation (7)), H_{quad}, (equation (8)) and H_{pol} (equation (9)) involve the products of angular integrals and of radial integrals. A semiquantitative estimate of the radial integrals for Rydberg electron–core dipole, quadrupole and anisotropic polarizability coupling for high n,n' non-penetrating ($l \geqslant 3$) states can be provided by the near-threshold approximation of Gilbert and Child [30], who used the asymptotic form of the phase shifted radial wavefunction

$$|n, l\rangle = \left(\frac{2}{\nu^3 r}\right)^{1/2} J_{2\lambda+1}((8r)^{1/2}), \tag{14}$$

where $\nu = n - \delta(l, \hat{\alpha})$, $\lambda = l - \delta(l, \hat{\alpha})$ is the effective azimuthal quantum number and $J(\cdot)$ is the Bessel function. The radial matrix elements of $r^{-(p+1)}$ (i.e. $p = 1$ for the dipole coupling (equation (7)), $p = 2$ for the quadrupole coupling (equation (8)) and $p = 3$

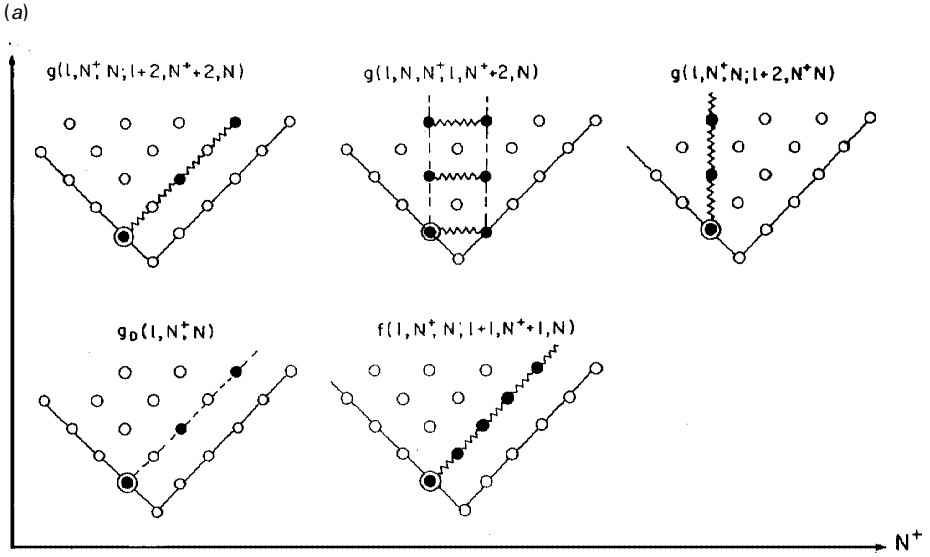

Figure 3(*a*) For legend see facing page.

for the anisotropic polarizability coupling (equation (9)) can be readily obtained using the standard integrals for the Bessel functions:

$$\langle n, l \left| r^{-(p+1)} \right| n', l' \rangle = \frac{a_0^{-(p+1)} 2^p \Gamma(2p-1)\, \Gamma(\lambda+\lambda'+2-p)}{(\nu\nu')^{3/2} \Gamma(\lambda+\lambda'+p+1)\, \Gamma(\lambda-\lambda'+p)\, \Gamma(\lambda'-\lambda+p)}, \qquad (15)$$

where $\Gamma(\cdot)$ is the gamma function. For dipole coupling ($p = 1$), equation (15) reduces to the Gilbert–Child [30] equation. In the appendix we provide the explicit expressions for the radial integrals obtained from equation (15) for the quadrupole ($p = 2$) and polarizability ($p = 3$) interactions.

The asymptotic results were applied for intramolecular long-range coupling between non-penetrating ($l \geqslant 3$) Rydberg states. The reliability of these asymptotic results is based on the analysis and numerical results for hydrogenic wavefunctions. For the hydrogenic wavefunctions we find that the asymptotic expressions provide a good approximation for the exact results for the multipole and polarizability integrals $\langle n, l \left| r^{-(p+1)} \right| n', l' \rangle$ ($p = 1, 2$ and 3) for large n, n'. We thus expect that the asymptotic expansion (equation (14)), in conjunction with the multipole and polarizability long-range interactions, provides an adequate description of the coupling, that is, the breakdown of the Hund coupling case (*d*), between non-penetrating ($l \geqslant 3$) high-n Rydberg states. In considering the limiting (high l) forms of the intramolecular couplings (equations (7)–(9)), we bear in mind that for the non-penetrating high-l orbitals the dominating contribution to the radial integrals $\langle nl \left| r^{-(p+1)} \right| n' l \pm q \rangle$ arises from the r domain outside the molecular ion core, where the asymptotic description of the phase shifted radial wavefunctions (equation (14)) is adequate. We shall utilize equations (A 1)–(A 11) for the matrix elements of $r^{-(p+1)}$ ($p = 1, 2, 3$) between high-l ($\geqslant 3$) non-penetrating states, which are characterized by small $\delta(l)$ values. These radial integrals, together with the general results given by equations (7)–(13), with the appropriate selection rules, provide explicit expressions for the long-range H_{dipole}, H_{quad} and H_{pol} intramolecular interactions.

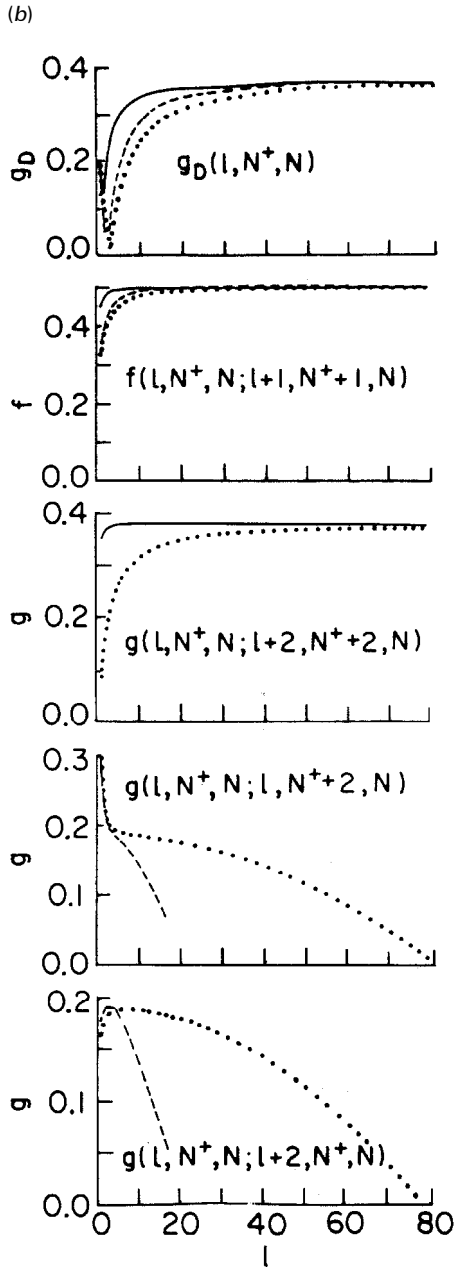

Figure 3. The angular integrals. (*a*) Schemes for the presentation of the angular momentum integrals. The $|n, l, N^+, N\rangle$ states are as follows: (⊙), doorway state; (●), states involved in diagonal and off-diagonal coupling; (○) other states. The strings mark the off-diagonal couplings. (i) $g_D(l, N^+, N)$ for $N^+ = N_I^+ + 2$, $l = l_I + 2$ and N is conserved. (ii) $f(l, N^+, N; l+1, N^+ + 1, N)$ for $N^+ = N_I^+ + 1$, $l = l_I + 1$ and N is conserved. (iii) $g(l, N^+, N; l+2, N^+ + 2, N)$ for $N^+ = N_I^+ + 2$, $l = l_I + 2$ and N is conserved. (iv) $g(l, N^+, N; l, N^+ + 2, N)$ for $l = l_I + 2$, N_0^+ is fixed and N is conserved $l \leqslant (N_0^+ + N)$. (v) $g(l, N^+, N; l+2, N^+, N)$ for $l = l_I + 2$, N_0^+ is fixed and N is conserved $l \leqslant (N_0^+ + N)$. (*b*) The l dependence of the angular integrals represented according to the schemes in (*a*): (——), $l_I = 1$, $N_I^+ = 0$, $N = 1$; (– – –), $l_I = 1$, N_I^+ (or N_0^+) = 9, $N = 10$; (· · · ·), $l_I = 1$, N_I^+ (or N_0^+) = 39, $N = 40$.

4. Model systems

Model calculations were performed for the energetics and for the intramolecular Rydberg electron–core dipole, quadrupole and anisotropic polarizability couplings for a real diatomic and for two model systems.

The generic example will involve the NO molecule, which constitutes the first molecule for which quantum defects were identified in the Rydberg level structure [51] and for which extensive spectroscopic and dynamic information [8, 9, 26, 33, 34, 51–72] on Rydberg states is available. The rotational constant for NO^+ is $B = 1{\cdot}9842\ cm^{-1}$ [8, 9]. To specify the Rydberg electron–core long-range interactions we need the core multipole moments, and the polarizability components γ and α of NO^+. The dipole moment of NO^+ was first calculated by Jungen and Lefebvre-Brion [73], giving $\mu = 0{\cdot}66 \pm 0{\cdot}38$ D. Recent experiments [74] and calculations [75] of the dipole moment of the $A\,^2\Sigma$ Rydberg state of NO resulted in $\mu = 1{\cdot}1$ D. We shall take the value of $\mu = 1{\cdot}0$ D (0·39 au) as a reasonable approximation. The quadrupole moment of NO^+ deduced by Jungen and Lefebvre-Brion [73] from the analysis of the lower nf ($n = 4, 5$) Rydberg states of NO was $Q = 0{\cdot}79 \pm 10^{-26} \pm 0{\cdot}08$ esu cm^2, in reasonable agreement with theoretical calculations, which resulted in the values $Q = 0{\cdot}62 \times 10^{-26}$ esu cm^2 [73] and $Q = 0{\cdot}56 \times 10^{-26}$ esu cm^2 [76]. We shall use the experimental value of $Q = 0{\cdot}79 \times 10^{-26}$ esu cm^2 (0·59 au). The isotropic polarizability of NO^+ is $\alpha = 1{\cdot}20 \times 10^{-24}$ cm^3 (8·17 au). The anisotropic polarizability of NO^+ was roughly estimated on the basis of experimental data of Bridge and Buckingham [77] for other diatomics as $\gamma = \alpha/2 = 0{\cdot}6 \times 10^{-24}$ cm^3 (4·1 au), which is somewhat higher than a previous estimate [73]. The $nf(N^+, N)$ and $ng(N^+, N)$ non-penetrating Rydberg states are characterized by the quantum defects $\delta(\mathrm{f}) = 0{\cdot}0101$ for $N^+ = 2$ and $N = 1$ [8, 9], $\delta(\mathrm{f}) = 0{\cdot}02$ for $N^+ = 3$ [8, 9] and $\delta(\mathrm{g}) \approx 3 \times 10^{-3}$ [66]. The l dependence of the quantum defects $\delta(l)$ for high l can be estimated from the diagonal matrix elements of the quadrupole and polarizability interactions [27]. Equations (8) and (9) give

$$\delta(l) = \frac{n^3}{2\mathrm{Ryd}}\left(\frac{\alpha e^2}{2}\langle n, l|r^{-4}|n, l\rangle + \frac{\gamma e^2}{3}\langle n, l|r^{-4}|n, l\rangle + eQ\langle n, l|r^{-3}|n, l\rangle\right) g_{\mathrm{D}}(l, N^+, N), \tag{16}$$

where $g_{\mathrm{D}}(l, N^+, N) = g(l, N^+, N; l, N^+, N)$. The diagonal angular integrals $g_{\mathrm{D}}(\cdot)$ (and other $g(\cdot)$ integrals) were evaluated using standard programs. For $l = 3$, one obtains, from equations (16), (A 9) and (A 10) for the ($N^+ = 2$) state $\delta(\mathrm{f}, N^+ = 2, N = 1) = 1{\cdot}7 \times 10^{-2}$, which is higher than the experimental value of $1{\cdot}01 \times 10^{-2}$ [8, 9]. For the f($N^+ = 3$) states $\delta(\mathrm{f}, N^+ = 3, N = 0) = 1{\cdot}8 \times 10^{-2}$, $\delta(\mathrm{f}, N^+ = 3, N = 1) = 1{\cdot}7 \times 10^{-2}$ and $\delta(\mathrm{f}, N^+ = 3, N = 2) = 1{\cdot}5 \times 10^{-2}$, which are lower by 10–25% than the experimental quantum defect $\delta(\mathrm{f}, N^+ = 3) = 2{\cdot}0 \times 10^{-2}$ [8, 9]. These deviations are presumably due to (small) penetration effects [34]. For higher values of $l\,(> 3)$ the quantum defect is

$$\delta(l) = \frac{3\alpha}{2a_0^3} l^{-5} + g_{\mathrm{D}}(l, N^+, N)\left(\frac{\gamma}{2a_0^3} l^{-5} + \frac{Q}{ea_0^2} l^{-3}\right). \tag{17}$$

For the NO data, equation (17) takes the numerical form $\delta(l) = 6{\cdot}1 l^{-5} + (2{\cdot}05 l^{-5} + 0{\cdot}59 l^{-3})\, g_{\mathrm{D}}(\cdot)$. The first term in $\delta(l)$ (equation (17)) dominates when $l < l_>$, where

$$l_> = \left(\frac{3\alpha e}{2a_0 Q g_{\mathrm{D}}(\cdot)}\right)^{1/2}. \tag{18}$$

The l dependence of the diagonal angular integrals will be presented using the following: N^+ increases from an initial value of N_I^+ by steps of $\Delta N^+ = 2$, while l increases from the initial value of l_I by steps of $\Delta l = 2$, and N is conserved (figure 3 (*a*)). The diagonal integrals of $g_D(l, N^+, N)$ for $N = 1$, $N_I^+ = 0$ for $N = 10$, $N_I^+ = 9$ and for $N = 40$, $N_I^+ = 39$ (figure 3 (*b*)) reveal a qualitatively similar behaviour and are almost constant, that is $g_D(\cdot) = 0{\cdot}36$, for large l.

From this analysis, in conjunction with equation (17) we conclude the following.

(1) For non-penetrating orbitals with moderately large values of $3 \leqslant l < l_>$ (with $l_> \approx 10$ being defined by equation (18)) the major contribution to the quantum defects originates from the isotropic polarizability, that is

$$\delta(l) \approx \frac{3\alpha}{2a_0^3} l^{-5}, l < l_>. \tag{19 a}$$

This result is well known from atomic Rydberg physics [49].

(2) For very large l values the (exceedingly small) quantum defect will be dominated by the quadrupole coupling. This state of affairs will be realized (except for pathological cases when $g_D \approx 0$) when $l > l_> = [3\alpha e/2a_0 Q g_D(\cdot)]^{1/2}$, that is $l_> \approx 10$ for most of the states of NO. The quantum defect is of the form

$$\delta(l) = \frac{Q}{ea_0^2} g_D(l, N^+, N)\, l^{-3}, l > l_>. \tag{19 b}$$

This result is of methodological interest for the characterization of the $\delta(l)$ for asymptotic large values of l.†

We also considered two model molecules. For a 'light' model molecule, the rotational constant is chosen as $B = 19\ \text{cm}^{-1}$, mimicking the features of a diatomic molecule containing a hydrogen atom. The quantum defects are taken from equation (17), and we took the NO multipoles and polarizability data. For a 'heavy' model molecule, the rotational constant is taken as $B = 0{\cdot}1$–$0{\cdot}05\ \text{cm}^{-1}$, which mimicks the features of Rydberg core–dipole coupling in a large molecule. The quantum defects are taken from equation (17), and we took again the NO multipoles and polarizability data.

5. Coupling and energy gaps between proximal pairs of high l ($\geqslant 3$) states

We explored the energetics and the n- and N^+-changing couplings of proximal (closest-lying) pairs of states. A proximal pair of states $|n, l, N^+, N\rangle$ and $|n', l', N^{+\prime}, N\rangle$ is chosen as follows.

(i) n, l, N^+ and N are fixed.

(ii) $l', N^{+\prime}$ and N are chosen to obey the appropriate selection rules, that is equation (11) for the dipole coupling, or equation (12) for the $\Delta N^+ = \pm 2$ quadrupole and anisotropic polarizability couplings.

(iii) n' is chosen to provide the smallest energy gap for this pair of states.

† The l^{-5} dependence ($l < l_<$) and l^{-3} dependence ($l > l_>$) of the quantum defect (equation (17)) originates from the first-order diagonal quadrupole and isotropic polarizability contributions for a rotating molecule. For an $l, m = 0$ Rydberg state in the field of a stationary dipole the second-order contribution to the quantum defect is $\delta(l) \propto l^{-3}$ [78, 79]. However, this situation corresponds to a rotator with an infinite moment of inertia, where the electronic angular momentum is conserved.

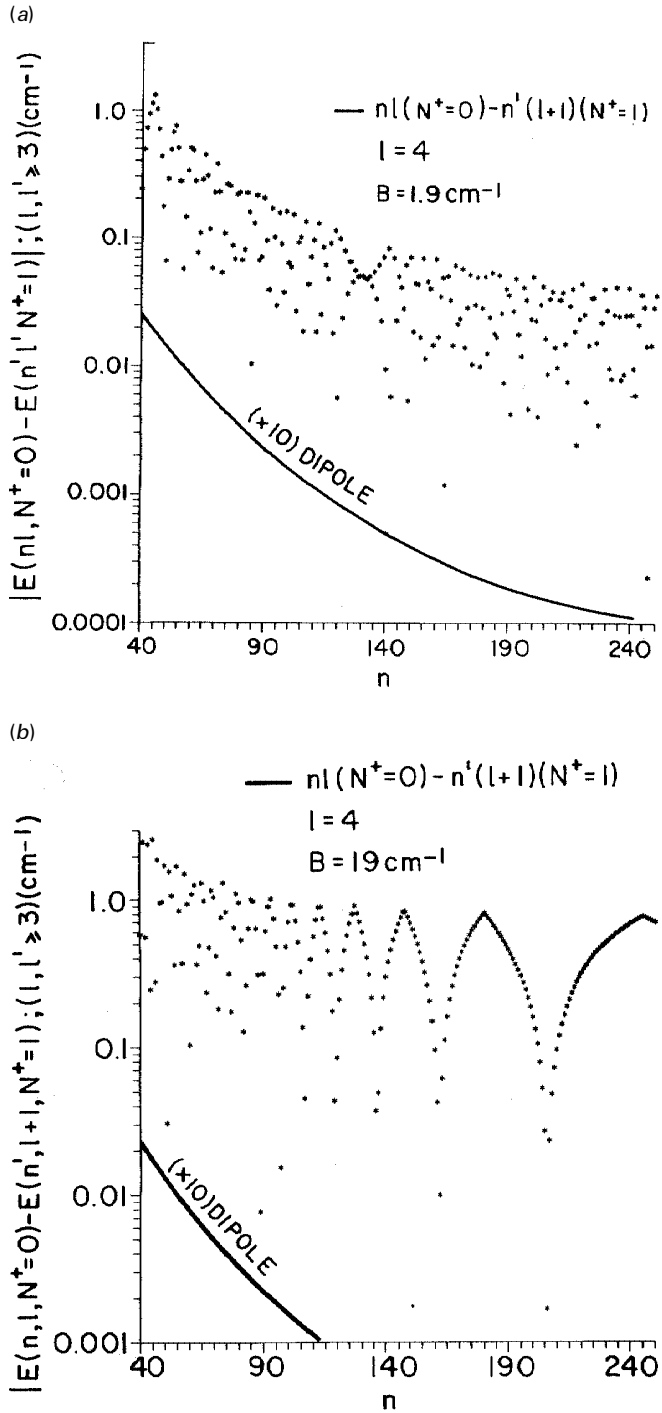

Figure 4(*a*, *b*) For legend see facing page.

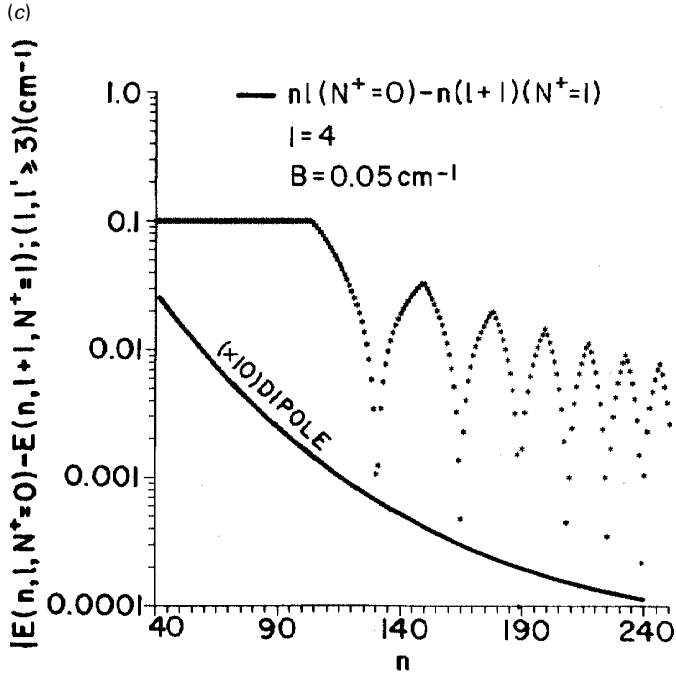

Figure 4. Energetics and coupling of proximal $nl\,(N^+ = 0)$ and $n'(l+1)\,(N^+ = 1)$ energy levels $(l \geqslant 3)$: (*a*) $B = 1{\cdot}9$ cm^{-1}; (*b*) $B = 19$ cm^{-1}; (*c*) $B = 0{\cdot}05$ cm^{-1}. The energy gaps between the $nl\,(N^+ = 0)$ state ($n = 40$–240) and the closest lying $n'(l+1)\,(N^+ = 1)$ state are marked by a point for each value of n. The solid line represents the dipole coupling matrix element (equation (21)) between the $l = 4$ and the $l = 5$ states.

The energy gaps will be subsequently compared with the exact and semiquantitative estimates of the strength of the corresponding intramolecular n- and N^+-changing couplings between these proximal pairs of states.

The n- and N^+-changing couplings involve all the allowed interactions for the dipole coupling ($\Delta N^+ = \pm 1$, with $\Delta l = \pm 1$) and the $\Delta N^+ = \pm 2$ (with $\Delta l = \pm 2$ and 0) couplings for the quadrupole and for the anisotropic polarizability interactions. The n' value for a given n ($n' \neq n$) is determined from equations (2) and (3) by the rotational constant and by the quantum defects. The energy gaps of the proximal pairs of states are numerically evaluated. We have examined the energy gaps $|E(n, l, N^+, N) - E(n', l', N^{+\prime}, N)|$ between pairs of proximal states in the range $n = 40$–240 for the non-penetrating $l\,(> 3)$ states. For the core rotation N^+ we have first chosen low values of $N^+ = 0$–3 (with $\Delta N^+ = \pm 1$ for dipole coupling and $\Delta N^+ = \pm 2$ for quadrupole and anisotropic polarizability couplings) for the NO molecule, for the 'light' model molecule and for the 'heavy' model molecule (section 4). Information on the behaviour of higher-N^+ states will be inferred from simple scaling of the low-N^+ data. Typical results for the energy gaps between proximal pairs of states are presented in figure 4 for the $nl(N^+ = 0) - n'(l+1)$ $(N^+ = 1)$, $(l \geqslant 3)$ pairs subjected to dipole coupling and in figure 5 for the $nl(N^+ = 0) \leftrightarrow n'(l+2)$ $(N^+ = 2)$, $(l \geqslant 3)$ pairs subjected to quadrupole or anisotropic polarizability couplings. These energy data reveal the following features.

(1) *Irregularity*. The energy gaps are irregular for the lower-n members of the $n = 40$–240 manifolds, with the upper limit of n for the irregular distribution

(*a*)

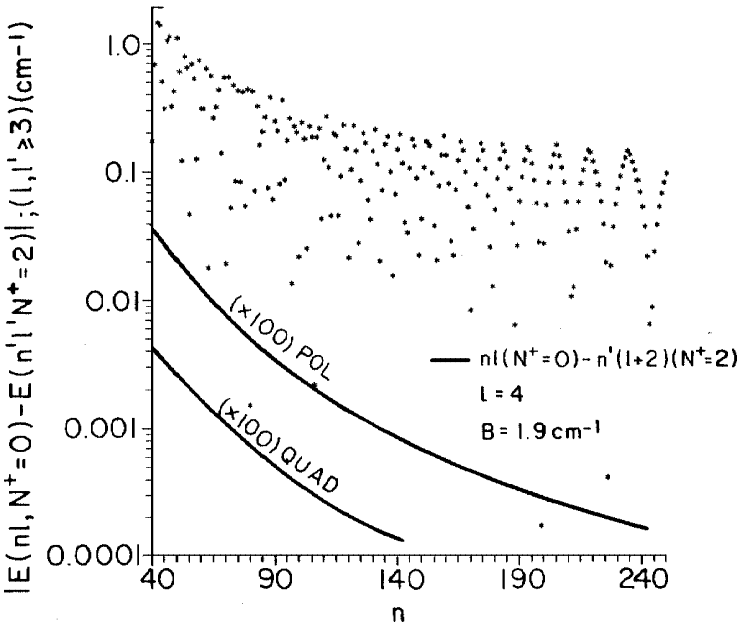

(*b*)

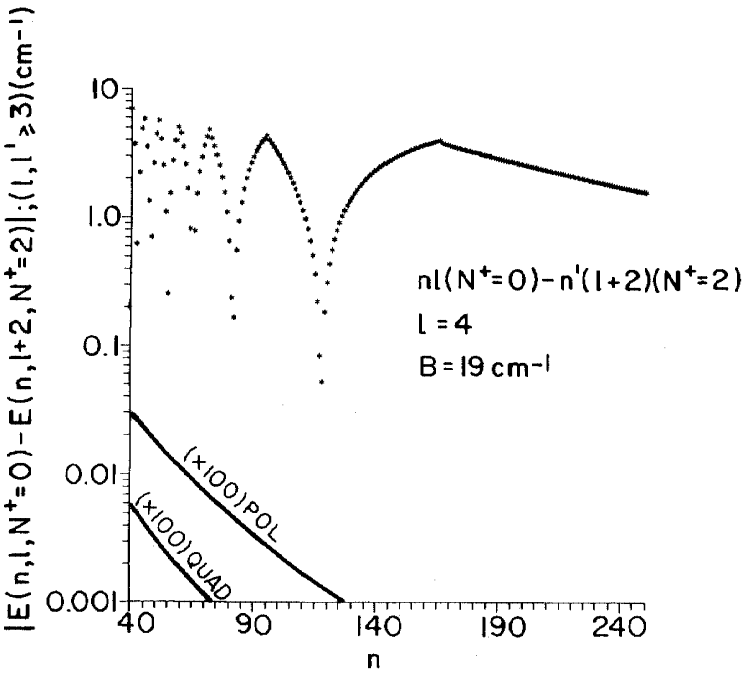

Figure 5(*a*, *b*) For legend see facing page.

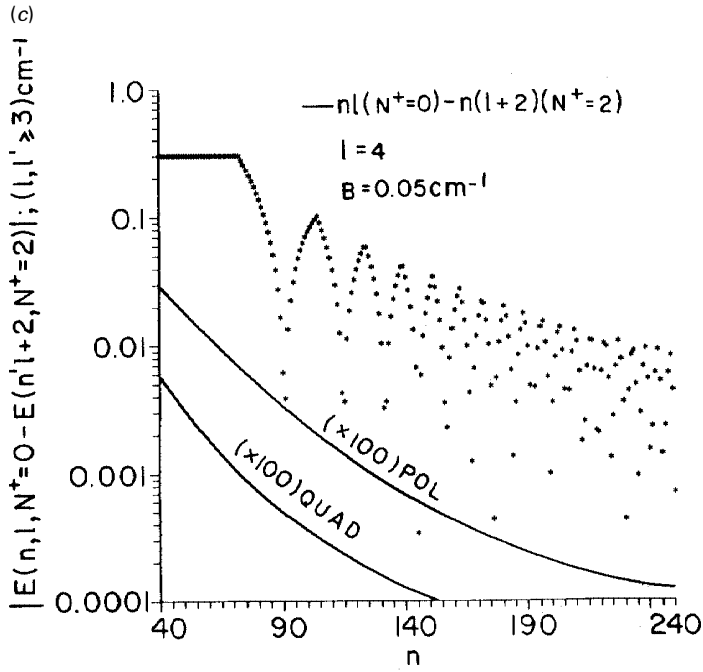

Figure 5. Energetics and couplings of proximal $nl(N^+ = 0)$ and $n'l'(N^+ + 2)$ energy levels ($l' - l = 2, 0$) for $l \geqslant 3$: (*a*) $B = 1{\cdot}9\ \mathrm{cm}^{-1}$; (*b*) $B = 19\ \mathrm{cm}^{-1}$; (*c*) $B = 0{\cdot}005\ \mathrm{cm}^{-1}$. The proximal energy gaps for $n = 40$–240 are marked by a point for each value of n. The two solid lines represent the $\Delta l = 2$ quadrupole (line labelled QUAD) coupling calculated from equation (24), and $\Delta l \neq 2$ anisotropic polarizability (line labelled POL) couplings calculated from equation (30) for the $l = 4 \rightarrow l = 6$ interaction.

becoming lower with decreasing B (figures 4 and 5). For a fixed value of B the majority of the energy gaps are higher for the quadrupole or polarizability coupling ($\Delta N^+ = \pm 2$) than for the dipole coupling ($\Delta N^+ = \pm 1$).

(2) *Resonance structure*. For higher values of n, the spectrum of the proximal energy gaps against n for both dipole and quadrupole or polarizability couplings reveals regularly spaced pronounced dips (figures 4 and 5). The onset of the structure occurs at lower n values for the low values of B ($= 0{\cdot}05\ \mathrm{cm}^{-1}$). These dips reflect the level structure of the sparser $\{|n', l', N^{+\prime}\rangle\}$ manifold ($N^{+\prime} > N^+$), which is given by equations (2) and (3) by $E(n', l', N^{+\prime}, N) = \Delta I(N^+; B) - \mathrm{Ryd}/[n - \delta(l')]^2$, where $\Delta I(N^+; B) = 2B(N^+ + 1)$ for dipole coupling and $\Delta I(N^+; B) = 2B(2N^+ + 3)$ for quadrupole or polarizability coupling. On the other hand, the denser manifold of higher-n ($> n'$) Rydberg states is $E(n, l, N^+, N) = -\mathrm{Ryd}/[n - \delta(l)]^2$. For large n values the dips, that is, the minimal energy gaps, are exhibited at each value of $E(n', l', N^{+\prime}, N)$.

(3) *Rotational energy scaling*. The energy gap spectra for $|E(n, l, N^+ = 0, N) - E(n', l + p, N^+ = p, N)|$ against n ($p = 1$ or 2) can be used to obtain the energy gap spectra $|E(n, l, N^+, N) - E(n', l + p, N^+ + p, N)|$, as the values of $\Delta I(N^+, B)$ presented above (point (2)) provide a convenient energy scaling. The energy gap spectrum for dipole coupling with $N^+ \leftrightarrow N^+ + 1$ in a molecule with a rotational constant B is isomorphous to the energy gap spectrum for $N^+ = 0 \leftrightarrow N^+ = 1$ with an effective rotational constant $B_{\mathrm{eff}} = B(N^+ + 1)$. Similarly, the

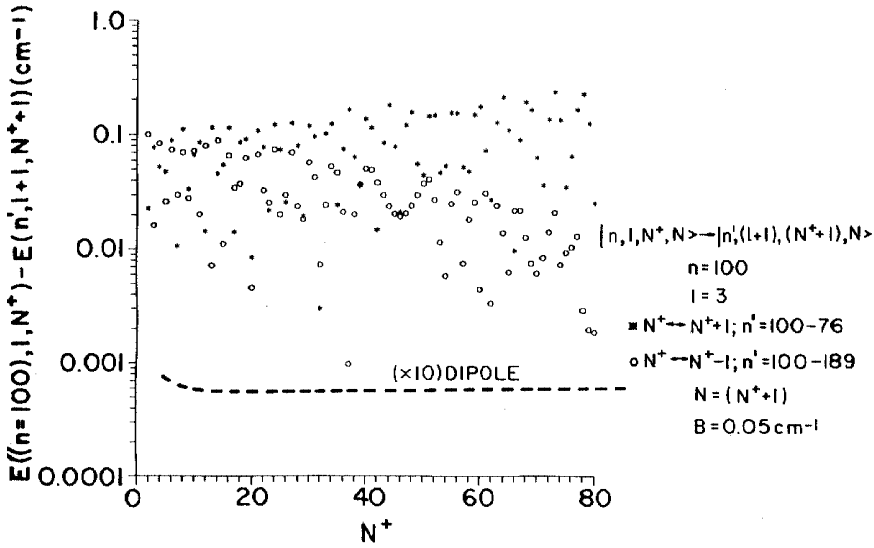

Figure 6. Energy gaps and couplings for the $|100, l, N^+, N\rangle$ and $|n', l+1, N^+ \pm 1, N\rangle$ proximal pairs of states ($l \geqslant 3$). The broken curve represents the calculated dipole coupling, (equation (7)) for a fixed $l = 3$ and for N^+ and $N = (N^+ + 1)$ varying in the range $N^+ = 3$–80.

energy gap for quadrupole or for polarizability coupling with $N^+ \leftrightarrow N^+ + 2$ in a molecule with a rotational constant B is analogous to the energy gap spectrum for $N^+ = 0 \leftrightarrow N^+ = 2$ with $B_{\text{eff}} = B(2N^+ + 3)$. This scaling procedure can be used to obtain the energy gap spectra at higher values of N^+ and at higher temperatures from the low-N^+ spectra.

(4) *Near-resonances.* The lowest values of the energy gaps between proximal pairs of states (figures 4 and 5) reveal two types of near-resonance: accidental near-resonances, which are completely random at lower values of n, and dips at the higher values of n.

(5) *The dependence of the energy gap spectra on B.* The overall values of the energy gaps (excluding accidental near-resonances) weakly increase with increasing B. The energy gaps at the dips also increase with increasing B.

(6) *The dependence of the energy gap spectra on the quantum defects.* Small (about 10%) changes in the quantum defects within a given 'l complex', which may originate from deviations from the Hund coupling case (d), do not affect the qualitative features of the proximal energy gap spectra. The gross features of the irregularity and of the resonance structure depend weakly on such changes in the quantum defects, while only the positions of accidental near-resonances are modified by such changes of $\delta(l)$.

(7) *The dependence of the energy gaps on N^+ and on the temperature.* The dependence of the energy gaps on N^+ (for fixed values of nl and l') is irregular over a broad range of N^+ values. This is apparent from the energy gap data for the $100l(N^+) - n'(l+1)(N^+ + 1)$ proximal pairs of states with a fixed value of $l \geqslant 3$ over the range $N^+ = 0$–80, for the heavy model molecule with $B = 0{\cdot}1$ cm^{-1} (figure 6). For this heavy model molecule the $N^+ \rightarrow (N^+ + 1)$ coupling spans the $n' = 76$–100 range while the $N^+ \rightarrow (N^+ - 1)$ coupling spans the $n' = 189$–100 range. The weak N^+ dependence of the energy gaps is in accord with

the scaling relations (section 3) which show that increasing N^+ results in the increase of B_{eff}, providing an overall weak increase in the energy gaps (point (5)). The value of $N^+ = 45$ corresponds to an effective temperature of about 300 K for this 'heavy' model molecule ($B = 0{\cdot}05\ \text{cm}^{-1}$), where high N^+ (about $(k_B T/2B)^{1/2}$) values can be accessible by optical excitation from a rotationally hot ground state at elevated temperatures. We thus conclude that temperature increase (resulting in a large increase of N^+) will not have a marked effect on the energy gaps.

The energy gaps between proximal pairs of states (with different N^+ values) will be now compared with the corresponding intramolecular couplings. The limiting high-l expressions for the radial integrals of the non-penetrating states (equations (A 1)–(A 3), and (A 5)–(A 11)) will be obtained by setting $l \gg 1$ and $\delta(l) \to 0$. The limiting high-l dipole coupling is obtained from equations (7) and (A 3) in the form

$$\langle n, l, N^+, N \left| H_{\text{dipole}} \right| n', l \pm 1, N^+ \pm 1, N \rangle = \frac{\mu e}{a_0^2} \frac{\Delta\delta(1)}{l} f(n, l, N^+, N; n', l \pm 1, N^+ \pm 1, N)\,(nn')^{-3/2}, \quad (20)$$

where $\Delta\delta(1)$ is the difference between the consecutive quantum defects (equation (A 4a)) and $f(\cdot)$ is the angular integral (equation (10)). In the high-l domain, $\delta(l)$ decreases with increasing l according to equations (17) and (19). The dominant contributions to $\delta(l)$ for high l are $\delta(l) = al^{-5}$ where $a = (3\alpha/2a_0^3)$ for $l < l_>$, and $\delta(l) = bl^{-3}$ where $b = (Q/ea_0^2)\, g_D(l, N^+, N)$ for $l > l_>$. Accordingly, we expect that $\Delta\delta(1) = 5a/l^6$ for $l < l_>$ and $\Delta\delta(1) = 3b/l^4$ for $l > l_>$. Thus the dipole interaction (equation (20)) decreases rapidly towards zero in the form

$$\langle n, l, N^+, N \left| H_{\text{dipole}} \right| n', l \pm 1, N^+ \pm 1, N \rangle = C_D (nn')^{-3/2} l^{-\eta_D}, \quad (21)$$

where

$$\begin{aligned} &\eta_D = 7,\ C_D = \frac{\mu e}{a_0^2} \frac{15\alpha}{2a_0^3} f(\cdot) && \text{for} \quad l < l_>, \\ &\eta_D = 5,\ C_D = \frac{\mu e}{a_0^2} \frac{3Qe}{ea_0^2} g_D(\cdot) f(\cdot) && \text{for} \quad l > l_>. \end{aligned} \quad (22)$$

The angular integrals $f(l, N^+, N; l+1, N^+ + 1, N)$ for the dipole couplings will be presented as follows (figure 3 (a)): N^+ and l increase from their initial values of N_I^+ and l_I respectively by steps of $\Delta N^+ = 1$ and $\Delta l = 1$, at fixed N. $f(\cdot)$ data for different values of N_I^+, l_I and N show similar behaviour (figure 3 (b)). $f(\cdot)$ is almost constant, that is $f(\cdot) = 0{\cdot}5$, for large values of l (figure 3 (b)). Taking again $g_D(\cdot) = 0{\cdot}36$ and the NO data we estimate that $C_D = 2{\cdot}6 \times 10^6\ \text{cm}^{-1}$ for $l < l_>$ and $C_D = 2{\cdot}7 \times 10^4\ \text{cm}^{-1}$ for $l > l_>$.

The N^+-changing high-l quadrupole couplings will be first considered for $\Delta l = \pm 2$ and $\Delta N^+ = \pm 2$, which results in direct l mixing. Equations (8) and (A 7) result in

$$\langle n, l, N^+, N \left| H_{\text{quad}} \right| n', l+2, N^+ + 2, N \rangle = \frac{Qe}{6a_0^3} \Delta\delta(2)\, g(l, N^+, N; l+2, N^+ + 2, N)\,(nn')^{-3/2} l^{-3}, \quad (23)$$

where $\Delta\delta(2)$ is defined by equation (A 8a), that is $\Delta\delta(2) = 10al^{-6}$ for $l < l_>$ and $\Delta\delta(2) = 6bl^{-4}$ for $l > l_>$. The $g(l, N^+, N; l+2, N^+ + 2, N)$ integrals are represented as follows (figure 3 (a)); N^+ and l increase from their initial values N_I^+ and l_I respectively

by steps of $\Delta N^+ = 2$ and $\Delta l = 2$, at fixed N. These $g(\cdot)$ integrals exhibit again similar behaviour for different values of N_I, l_I and N (figure 3(*b*)). $g(\cdot)$ is almost constant, that is $g(\cdot) = 0{\cdot}35$ for large values of l (figure 3(*b*)). These N^+- and l-changing quadrupole interactions decrease rapidly to zero as

$$\langle n, l, N^+, N \left| H_{\text{quad}} \right| n', l+2, N^+ + 2, N \rangle = C_Q (nn')^{-3/2} l^{-\eta_Q}, \tag{24}$$

where

$$\begin{aligned} \eta_Q &= 9, \; C_Q = \frac{Qe}{a_0^3} \frac{5\alpha}{2a_0^3} g(\cdot) \qquad \text{for} \quad l < l_>, \\ \eta_Q &= 7, \; C_Q = \frac{Q^2}{2a_0^5} g(\cdot)\, g_D(\cdot) \quad \text{for} \quad l > l_>. \end{aligned} \tag{25}$$

For the NO input data of section 4 we estimate $C_Q = 9{\cdot}3 \times 10^5 \text{ cm}^{-1}$ for $l < l_>$ and $C_Q = 4{\cdot}8 \times 10^3 \text{ cm}^{-1}$ for $l > l_>$.

For completeness we present the expressions for $\Delta l = 0$ ($\Delta N^+ = 2$) quadrupole couplings for large values of l, which are given by

$$\langle n, l, N^+, N \left| H_{\text{quad}} \right| n', l, N^+ + 2, N \rangle = \frac{Qe}{a_0^3} g(l, N^+, N; l, N^+ + 2, N) (nn')^{-3/2} l^{-3}. \tag{23a}$$

The l-conserving $g(l, N^+, N; l, N^2 + 2, N)$ integrals will be represented using the following scheme (figure 3(*a*)): N is conserved, $N^+ = N_0^+$ is fixed, l increases from the initial value of l_I by steps of $\Delta l = 2$ to the upper limit $l \leqslant N_0^+ + N$. These angular integrals $g(\cdot)$ (figure 3(*b*)) can be scaled for different values of N_0^+ and N and can be approximately represented by

$$\begin{aligned} g(\cdot) &\approx 0{\cdot}15, \qquad\qquad l < \frac{N_0^+ + N}{2}, \\ g(\cdot) &\approx 0{\cdot}15 \frac{(N_0^+ + N)^2}{4} l^{-2}, \quad l > \frac{N_0^+ + N}{2}, \end{aligned} \tag{26}$$

where N_0^+ and N characterize the doorway state. For sufficiently large values of l we estimate for $\Delta l = 0$ coupling $\langle n, l, N^+, N \left| H_{\text{quad}} \right| n', l, N^+ + 2, N \rangle \approx C_Q^{(0)} (nn')^{-3/2} l^{-5}$, where $C_Q^{(0)} \approx 0{\cdot}15 (Qe/a_0^3)(N_0^+ + N)^2/4$, that is $C_Q^{(0)} = 1{\cdot}9 \times 10^4 (N_0^+ + N)^2/4 \text{ cm}^{-1}$. This $\Delta l = 0$ large-l quadrupole coupling is independent of the quantum defect. The $\Delta l = 0$ quadrupole coupling (proportional to l^{-5}), although considerably larger than the $\Delta l = \pm 2$ coupling (proportional to l^{-9} for $l < l_>$ and proportional to l^{-7} for $l > l_>$), does not result in direct l mixing and still decreases rapidly with increasing l.

Equations (22) and (24) for the dipole coupling and for the ($\Delta l = \pm 2$) quadrupole couplings for large l imply the vanishing of the radial integrals for these l-changing multipole interactions in the limit of vanishing quantum defects, that is

$$\langle n, l \left| r^{-(p+1)} \right| n', l \pm p \rangle = 0, \quad p = 1, 2, \quad \delta(l) = 0. \tag{27}$$

Equation (27) is consistent with an exact general relation for Laguerre polynomials [80–82], which implies that for radial hydrogenic wavefunctions within a single n manifold

$$\langle n, l \left| r^{-(p+1)} \right| n, l \pm p \rangle = 0 \tag{28}$$

for integer $p \geqslant 1$. Equation (28) was proven by Feinberg [80] for $p = 1$ and by

Pasternack and Sternheimer [81] for the general case using the generating function for the Laguerre polynomials. Armstrong [82] advanced group theory to show that the hydrogenic radial wavefunctions form bases for the irreducible unitary representations of an algebra isomorphic to that of the O(2, 1) group. This group theoretical analysis resulted in the selection rule in equation (28) [82]. We note that, while the exact relation, equation (28), implies the vanishing of the integrals only within the same n manifold, the asymptotic relation, equation (27), also implies the vanishing of the integrals for dipole coupling between different n manifolds, as the r dependence of the near-threshold wavefunction is independent of n, being determined only by l.

We now turn to the limiting high-l form of the anisotropic polarizability interaction (equations (9) and (A 11)). For the anisotropic polarizability coupling for large l both the $\Delta l = \pm 2$ and the $\Delta l = 0$ interactions are characterized by the same radial integral, (equation (A 11)). The anisotropic polarizability coupling for N^+-changing $\Delta l = \pm 2$ is

$$\langle n, l, N^+, N \left| H_{\mathrm{pol}} \right| n, l+2, N^++2, N \rangle = \frac{\gamma e^2}{12 a_0^4} (nn')^{-3/2} g(l, N^+, N; l+2, N^++2, N)\, l^{-5}. \tag{29}$$

On the basis of the numerical results (figure 3(b)) for the $g(l, N^+, N; l+2, N^++2, N)$ integral in equation (29) (represented according to the scheme in figure 3(b)), we take the nearly constant value of $g(\cdot) = 0{\cdot}35$, resulting in the $\Delta l = \pm 2$, $\Delta N^+ = \pm 2$ anisotropic polarizability interaction

$$\langle \left| H_{\mathrm{pol}} \right| \rangle = C_{\mathrm{P}} (nn')^{-3/2} l^{-5}, \tag{30}$$

where $C_{\mathrm{P}} = (\gamma e^2/12 a_0^4)\, g(\cdot)$, so that $C_{\mathrm{P}} = 2{\cdot}6 \times 10^4$ cm^{-1}. For the $\Delta l = 0$, $\Delta N^+ = \pm 2$ anisotropic polarizability the interaction is of the same form as equations (29) and (30) with the angular integral being replaced by $g(l, N^+, N; l, N^++2, N)$. This angular integral (figure 3(b)) is approximated by equation (26). Accordingly, for large l and $\Delta l = 0$ the polarization interaction is

$$\langle n, l, N^+, N \left| H_{\mathrm{pol}} \right| n, l, N^++2, N \rangle = C_{\mathrm{P}}^{(0)} (nn')^{-3/2} l^{-7}, \tag{31}$$

where $C_{\mathrm{P}}^{(0)} \approx (\gamma e^2/12 a_0^4)\, 0{\cdot}15 (N_0^+ + N)^2/4$. The $\Delta l = 0$ polarizability interaction, which does not result in l mixing, exhibits a faster decrease with increasing l than does the corresponding l-changing interaction.

We note that the general structures of the high-l dipole and $\Delta l = \pm 2$ quadrupole interactions (equations (21) and (24)) are $\Delta\delta_l(p)\, l^{-(\beta+\gamma)}$, containing the quantum defect difference $\Delta\delta_l(p)$, the contribution β of the radial integral and the contribution γ of the angular integral. For the dipole interaction $p = 1$, $\beta = 1$ and $\gamma = 0$ while for the $\Delta l = \pm 2$ quadrupole interaction $p = 2$, $\beta = 3$ and $\gamma = 0$. The $\Delta l = 0$ quadrupole and the $\Delta l = \pm 2, 0$ polarizability interactions are of the form $l^{-(\beta+\gamma)}$, being independent of $\Delta\delta_l(P)$, with $\beta = 3$, $\gamma = 2$ for the $\Delta l = 0$ quadrupole, $\beta = 5$, $\gamma = 0$ for the $\Delta l = \pm 2$ polarizability and $\beta = 5$, $\gamma = 2$ for the $\Delta l = 0$ polarizability coupling.

The n- and N^+-changing interactions involving non-penetrating ($l \geqslant 3$) high-n states are characterized as follows.

(1) *Hierarchy of different l-changing interactions.* For the non-penetrating states the dipole ($\Delta N^+ = 1$) coupling (for typical values of $\mu = 1$ D for a polar molecule) dominates over the quadrupole ($\Delta l = \pm 2$) coupling (with a typical value of $Q = 1{\cdot}0 \times 10^{-26}$ esu cm^2) from the same $|nlN^+\rangle$ state (figures 4 and 5). The $\Delta l = \pm 2$ anisotropic polarizability coupling seems to be larger than the

$\Delta l = \pm 2$ quadrupole coupling for the same pair of states. Although the strength of the H_{pol} coupling is determined by the anisotropic polarizability γ, which is unknown for NO^+, we believe that our crude estimate of $\gamma(\approx 4{\cdot}1$ au) is reasonable both for NO and for the other model molecules considered herein.

(2) *The* $\Delta l = 0$ *interactions*. The $\Delta l = 0$ $(0 \leftarrow\!\!\!/\!\!\!\rightarrow 0)$ $nl(N^+) - n'l(N^+ + 2)$ quadrupole interactions (proportional to l^{-5}) are large, compared with the corresponding $\Delta l = \pm 2$ interactions from the same $nl(N^+)$ state, owing to the stronger l power dependence of the latter interaction. On the other hand, the $\Delta l = 0$ anisotropic polarizability interactions (proportional to l^{-7}) decrease more rapidly than the corresponding $\Delta l = 2$ interaction (proportional to l^{-5}) for large l. These $\Delta l = 0$ quadrupole and anisotropic polarizability interactions do not result in direct l mixing (figures 1 and 2) and can be involved in mediated (higher-order) coupling.

(3) *Power-law dependence of the high-l intermolecular interactions*. All the intermolecular interactions are of the form proportional to $l^{-\eta}$. These interactions are characterized by $\eta = 7$ $(l < l_>)$ and $\eta = 5$ $(l > l_>)$ for the dipole coupling, $\eta = 9$ $(l < l_>)$ and $\eta = 7$ $(l > l_>)$ for the $\Delta l = \pm 2$ and N^+-changing quadrupole coupling, $\eta = 3$ $(l < (N_+ + N)/2)$ and $\eta = 5$ $(l > (N_+ + N)/2)$ for the l-conserving quadrupole interaction, $\eta = 5$ for the l-changing polarizability interaction and $\eta = 7$ for the l-conserving polarizability interaction. All the high l intermolecular interactions decrease rapidly with increasing l.

(4) *n- and* N^+*-changing interactions and proximal energy gaps*. From the comparison of the proximal energy gaps between the pairs of states $|n, l, N^+, N\rangle$ and $|n', l+P, N^++P, N\rangle$ (at fixed N^+) with the dipole ($\Delta l = \pm 1$), quadrupole and polarizability ($\Delta l = \pm 2, 0$) couplings for non-penetrating ($l \geqslant 3$) high-n, n' Rydberg states (figures 4 and 5) we conclude that all the energy gaps ΔE are very large (i.e. by one to two orders of magnitude for the NO molecule and for the model molecules considered herein) relative to the corresponding couplings. A similar situation prevails for high-N^+ states, which are accessible for optical excitation from a rotationally hot ground state at $T = 300$ K. In figure 6 we present the N^+ dependence of the dipole couplings (equation (7)) between proximal pairs of states $|n, l, N^+, N\rangle$ and $|n', l+1, N^+ \pm 1, N\rangle$ with fixed l $(= 3)$, and with N^+ being changed in the range $N^+ = 3$–80 and $N = N^+ + 1$. Again the energy gaps ΔE exceed (by more than an order of magnitude) the $l = 3 - l = 4$ dipole coupling, which falls off (proportional to l^{-7}) at higher values of l. We thus conclude that, for the high-n non-penetrating states,

$$\frac{|\langle n, l, N^+, N| H_{int} |n', l \pm p, N^+ \pm q, N\rangle|}{|\Delta E|} \ll 1 \tag{32}$$

for $H_{int} = H_{dipole}(p = q = 1)$, $H_{quad}(p = 2, 0$ and $q = 2)$ and $H_{pol}(p = 2, 0$ and $q = 2)$.

We infer that the fast decrease in the n- and N^+-changing intramolecular interactions with increasing l prohibits intramolecular mixing of these states within the high-l $(\geqslant 3)$ manifold, whereupon n and N^+ mixing (via both l-changing and l-conserving interactions) is prohibited. What remains to be done in the realm of the exploration of intramolecular interactions for high-n Rydberg states is to examine the consequences of quadrupole and anisotropic polarizability coupling for N^+-conserving ($\Delta N^+ = 0$) interactions.

6. N^+-conserving energetics and couplings within a single n manifold

The quadrupole and anisotropic polarizability couplings with $\Delta N^+ = 0$ ($\leftarrow/\rightarrow 0$) and $\Delta l = \pm 2$ involve pairs of states within a single n manifold, that is, for the high-l ($\geqslant 3$) non-penetrating states one takes the nl states with the fixed N. The energy gaps within a single n manifold are determined by the quantum defects, being independent of the rotational constant. Such a manifold of N^+-conserving states is limited according to equation (13) to the region of l states $|N - N| \leqslant l \leqslant (N + N^+)$.

In the high-l (> 3) domain the energy gaps for the states $|n, l, N^+\rangle$ and $|n, l+2, N^+\rangle$ are $\Delta E(l; l+2) = (2\mathrm{Ryd}/n^3)\,\Delta\delta_l(2)$. Making use of the limiting high-l relations for the quadrupole and polarizability couplings we can estimate the ratios of the couplings and the energy gaps. For the quadrupole interaction the ratio of coupling to energy gap is

$$r_Q = \frac{\langle n, l, N^+, N\,|H_{\mathrm{quad}}|\,n', l+2, N^+, N\rangle}{\Delta E(l; l+2)}$$

$$= \frac{Q}{6ea_0^2}\, g(l, N^+, N; l+2, N^+, N)\, l^{-3}. \tag{33}$$

The $g(l, N^+, N; l+2, N^+, N)$ integral (figure 3 (*b*)) at fixed values of (N^+, N) (figure 3 (*a*)) and for larger values of l is expected to be similar to the $g(l, N^+, N; l, N^+ + 2, N)$ integral. This expectation is borne out by the data in figure 3. The angular integral $g(\cdot)$ in equation (33) is given by equation (26) with $g(\cdot) = 0$ for $l > (N_+ + N)$. The ratio (33) is

$$\begin{aligned} r_Q &= 0{\cdot}15\,\frac{Q}{6ea_0^2}\, l^{-3}, && l < \frac{N^+ + N}{2}, \\ r_Q &= 0{\cdot}15\,\frac{Q}{6ea_0^2}\,\frac{(N+N^+)^2}{4}\, l^{-5}, && \frac{N^+ + N}{2} < l \leqslant N^+ + N. \\ r_Q &= 0 && l > N^+ + N. \end{aligned} \tag{34}$$

As the numerical factor in equation (34), $0{\cdot}15(Q/6ea_0^2) = 1{\cdot}5 \times 10^{-2}$, is small we infer the following.

(1) The n- and N^+-conserving quadrupole couplings are small relative to the energy gaps and this ratio falls off rapidly with increasing l, that is $\propto l^{-3}$ for $l < (N^+ + N)/2$, and $\propto l^{-5}$ for $(N^+ + N)/2 < l \leqslant (N^+ + N)$. Angular momentum conservation implies the vanishing of this coupling for $l > (N^+ + N)$.

For the anisotropic polarizability coupling, we have for the ratio of coupling to energy gap

$$r_P = \frac{\langle n, l, N^+, N\,|H_{\mathrm{pol}}|\,n', l+2, N^+, N\rangle}{\Delta E(l; l+2)}$$

$$= \frac{\gamma}{12a_0^3\,\Delta\delta_l(2)}\, g(l, N^+, N; l+2, N^+, N)\, l^{-5}. \tag{35}$$

The $g(\cdot)$ integrals in equation (35), which are schematically presented in figure 3 (*a*), will again be represented by equation (26) for $l \leqslant (N^+ + N)$ and vanish for

$l > (N^+ + N)$, where N^+ and N are fixed. $\Delta\delta_l(2)$ for $l < l_>$ and for $l > l_>$ is given in section 5. For small values of $(N^+ + N)$, that is $l_> > (N^+ + N)$ we have

$$r_P = 8 \times 10^{-4} \frac{\gamma}{\alpha} \frac{(N^+ + N)^2}{4} l^{-1}, \qquad l < N^+ + N,$$
$$r_P = 0, \qquad 1 > N^+ + N. \tag{36}$$

For large values of $N^+ + N$, that is $l_> < (N^+ + N)/2$ we have for large l

$$r_P = \frac{e\gamma}{Q a_0 g_D} 2 \times 10^{-4} \frac{(N^+ + N)^2}{4} l^{-3}, \qquad l > \frac{N^+ + N}{2}$$
$$r_P = 0, \qquad l > N^+ + N. \tag{37}$$

From this analysis of the polarizability coupling for N^+-preserving interactions at high l values we conclude the following.

(2) The n- and N^+-conserving anisotropic polarizability coupling for high l is small relative to the energy gaps, and their ratio falls off (proportional to l^{-1} or proportional to l^{-3}) with increasing l. Again angular momentum conservation implies that these couplings are limited to the range $l \leqslant (N^+ + N)$.

7. Concluding remarks

7.1. *The bottleneck effect for intramolecular electron–core coupling*

We have established the characteristics of the intramolecular dipole, quadrupole and anisotropic polarizability couplings in the absence of an electric field. A central conclusion emerging from our analysis for l (> 3) non-penetrating Rydberg states is that the intramolecular interactions decrease rapidly towards zero as $l^{-\eta}$. The powers η are determined by the l dependence of the nature of the interaction, of the quantum defect (for the multipole interaction) and of the angular integral. Concurrently, the energy gaps for proximal pairs of states subjected to N^+-changing ($n' \neq n$) coupling are large relative to the $l \geqslant 3$ dipole, quadrupole and anisotropic polarizability interactions. For N^+-conserving interactions within a single n manifold the energy gaps decrease as $l^{-\xi}$, that is, $\xi = 6$ ($l < l_>$) and $\xi = 4$ ($l > l_>$), with $\eta > \xi$ resulting in a negative power law of the form $l^{-|\eta - \xi|}$ for the coupling-to-energy gap ratios.

Our analysis of the intramolecular coupling and dynamics of high-n non-penetrating Rydberg states rests on the representation of the zero-order basis set by the Hund coupling case (d) and the incorporation of long-range multipole and polarizability interactions. We have proven that, for non-penetrating ($l \geqslant 3$) Rydberg states, firstly for n- and N^+-changing interactions the coupling is much less than the energy gap and secondly for n- and N^+-conserving interactions the coupling-to-energy gap ratio is proportional to $l^{-|\eta - \xi|} \to 0$. These results rest on the asymptotic high-l behaviour of the components of the intramolecular coupling, in conjunction with the characteristics of the energy gaps between proximal pairs of states. Our analysis establishes the existence of a bottleneck effect, which precludes 'global' l mixing by Rydberg electron–core intramolecular interactions. The implications of the bottleneck effect for high-n ($l \geqslant 3$) Rydberg states are as follows.

(1) For N^+-changing coupling ($n' \neq n$), 'global' intramolecular l mixing in conjunction with electronic–rotational energy exchange (i.e. $nN^+ - n'(N^+ \pm p)$ coupling) is prohibited.

(2) For N^+-conserving coupling within a single l manifold for $l \leqslant (N^+ + N)$ 'global' l mixing is prohibited.

It is important to emphasize that our demonstration of the bottleneck effect depends on the characteristics of the intramolecular couplings of the non-penetrating states, which are invariant with respect to the magnitude of the rotational constants. As far as the energetics are concerned, the large magnitude of most proximal energy gaps for N^+-changing interactions is not very sensitive to the rotational constant B (although some decrease in these energy gaps with decreasing B is exhibited), while the energy gaps for N^+-conserving interactions are independent of B. We thus infer that the bottleneck effect for intramolecular coupling is expected to be universal both in a diatomic molecule and for a large molecule.

7.2. *Implications*

What are the dynamic and spectroscopic implications of the intramolecular Rydberg electron–core interactions?

(1) 'Global' l mixing cannot be induced by (field-free) intramolecular coupling. We have provided an answer to a central question in the realm of the dynamics of high-n Rydberg states. What is the coupling responsible for the 'global' l mixing which results in the dramatic lifetime dilution effect? Our analysis of the bottleneck effect, which is general both for diatomics and for large molecules, implies that Rydberg lifetime dilution effects within the entire l manifold cannot be due to intramolecular coupling and can be induced only by exterior electric field coupling [15–17, 22–26].

(2) Intramolecular (field-free) interactions induce the mixing of some pairs of low-l states. These interactions between low ($l < 3$) penetrating orbitals fall into two categories: firstly extensive l–l' mixing for all n, which prevails for the s–d mixing in NO [33], which cannot be handled by multipole and polarizability interactions, with the Hund coupling case (b) providing a more suitable basis for this problem [33]; secondly accidental near-resonances, which involve all the other intramolecular interactions between penetrating ($1 \leqslant l \leqslant 3$) states of NO (and other diatomic molecules). Typical examples are the p–d dipole coupling and the p–f quadrupole and polarizability coupling in NO, being characterized by a few (about 10% of the states in the range n = 40–240) accidental near-resonances [26]. These near-resonance effects for high-n (> 40) $1 \leqslant l \leqslant 3$ Rydberg states are rare. The mixing of states characterized by small energy gaps $\Delta E \leqslant \langle H_{\text{int}} \rangle$ relative to the coupling will result in the redistribution of the decay widths between the pair of states. The dynamic implications of such local perturbations will be manifested in either the shortening or lengthening of the lifetime of the doorway state (for excitation) depending on the decay widths of the $|n, l, N^+\rangle$ and $|n', l', N^{+\prime}\rangle$ states. The spectroscopic implication of such near-resonant coupling may be manifested in the appearance of satellite bands in absorption, when the transition probability to the $|n', l', N^{+\prime}\rangle$ states is weak. In this context, Gilbert and Child [30] have demonstrated the spectroscopic effects of intramolecular dipole coupling with a Rydberg 'quasicontinuum' [30]. This interesting problem of the characterization of the electronic Rydberg 'quasicontinuum' will be discussed elsewhere [83].

(3) Mediation can occur by simultaneous (low-l) intramolecular and electric field coupling. In the presence of a weak (stray or imposed) electric field (F = 0·05–1 V cm^{-1}) some low-l (< 3) core-penetrating states characterized by modest energy gaps, that is $\langle H_{int} \rangle \lesssim |E(n,l,N^+) - E(n',l',N^{+\prime})|$, act as mediating states for electric field-induced coupling of the doorway state $|n,l,N^+\rangle$ with the $|n',l''(>3),N^+\rangle$ manifold. Intramolecular coupling in conjunction with Stark coupling H_{stark} results in the mediated-sequential scheme

$$|n,l,N^+\rangle \xleftrightarrow{H_{int}} |n', l = 2l+p, N^{+\prime} = N^+ \pm p\rangle\ (p = 1,2) \xleftrightarrow{H_{stark}}$$

$$|n', l'+1, N^{+\prime}\rangle \xleftrightarrow{H_{stark}} |n', l'+2, N^{+\prime}\rangle \xleftrightarrow{H_{stark}} \ldots .$$

Two notable examples of Rydberg states subjected to mediated-sequential intramolecular (dipole) and electric field couplings involve the

$$92\mathrm{p}(N^+ = 0) - 80\mathrm{d}(N^+ = 1) - \{80, l'' > 3\,(N^+ = 1)\}$$

and $95\mathrm{p}(N^+ = 0) - 82\mathrm{d}(N^+ = 1) - \{|92, l'' > 3\,(N^+ = 1)\}$ manifolds of NO [9, 26].

7.3. *What about huge molecules and clusters?*

Regarding the applicability of our model to high-n Rydberg states of huge molecules, for example, large aromatic molecules, and of molecular clusters, we can infer that the ion core dipole moment and also the ion core quadrupole moment will be similar for the diatomic and for the huge molecules and clusters. It should be noted, however, that for dipole and for ($\Delta l = \pm 2$) quadrupole coupling large $l < l_> = 3\alpha e/2a_0 Q$ couplings are determined by the quantum defect differences, $\Delta\delta(p) \propto \alpha$ ($p = 1, 2$), which are in turn determined by the isotropic polarizability. α will be considerable larger for large molecules, that is $\alpha = 10{\cdot}4$ Å^3 for benzene [77] and is larger by about one order of magnitude for very large aromatics and for large clusters. One thus expects that $l_> \propto \alpha$ is very large for large aromatic molecules, so that only the range $l < l_>$ will prevail in these systems. For the dipole interaction the coupling is $\mu\Delta\delta(1)l^{-1} \propto \mu\alpha l^{-7}$ (for $l < l_>$), while for the N^+- and l-changing quadrupole interaction the coupling is $Q\Delta\delta(2)l^{-3} \propto Q\alpha l^{-9}$ ($l < l_>$). For a given value of l these multipole couplings are considerably larger than for diatomic molecules. A similar situation may prevail for the anisotropic polarizability interaction of planar aromatic molecules γl^{-5}, as γ is expected to scale with α, being larger by one to two orders of magnitude than for diatomic molecules. On the other hand, for one-component elemental and molecular clusters, γ is small, while large values of γ may prevail for some heteroclusters, for example an aromatic molecule solvated by rare-gas atoms. A cursory examination of figures 4 and 5 indicates that for a large aromatic molecule characterized by a polarizability $\alpha \approx 100\alpha(\mathrm{NO})$ and $\gamma \approx 100\gamma(\mathrm{NO})$, where $\alpha(\mathrm{NO}) = 8{\cdot}2$ au and $\gamma(\mathrm{NO}) \approx 4{\cdot}1$ au, the dipole $l = 4$ to $l = 5$ interactions will involve a modest number (10%) of accidental or dip-type near-resonances, while for $l = 4$ to $l = 6$ quadrupole and polarizability couplings the number of near-resonances is small. Of course, for higher l values, that is, $l > 5$, the number of near-resonances is negligible for all interactions. These arguments imply the following for non-penetrating Rydberg states in large molecules.

(1) The quantum defects for a given value of nearly non-penetrating high l are considerably larger for aromatic than for diatomic molecules.

(2) Some intramolecular near-resonance couplings may prevail for *n*f and *n*g orbitals.
(3) For $l > 5$ Rydberg states the non-penetrating Rydberg states are decoupled and no intramolecular l mixing occurs.

Arguments (1) and (2) are heuristic, as for large molecules some core penetration will prevail also for $l = 3$–4 Rydberg states. Point (3) is of importance as it implies the universality of the bottleneck effect from diatomic molecules to very large molecules and clusters.

Another aspect of the Rydberg dynamics of large molecules and clusters pertains to the nature of the intramolecular decay channels. While in diatomic molecules the non-radiative decay channels involve pre-dissociation and autoionization, for large molecules the internal conversion channel sets in. Regarding the decay of high-*n* Rydberg states in large molecules via internal conversion several possibilities come to mind.

(i) Direct decay of Rydberg states to intravalence electronic–vibrational excitations.
(ii) Mediated decay of high-*n* Rydberg states via coupling to vibrationally excited lower-*n* Rydberg state(s) to the final intravalence electronic–vibrational excitation.

Mechanism (ii) provides an analogue to mediated internal conversion and intersystem crossing between intravalence excitations [84]. Of course, the mediated decay of a high Rydberg state may involve several lower-*n* Rydberg states, exhibiting energy disposal by cascading between several Rydberg states of decreasing *n*. Such a mediated Rydberg internal conversion is expected to exhibit deviations from the n^3 scaling law for the non-radiative decay time of the doorway *n* Rydberg state, as on changing *n* the nature of the mediating states is changed. Deviations from the n^3 scaling law in large molecules were experimentally reported [7] for the non-radiative lifetimes of the $n = 10$–20 Rydberg states of 1,4-diazabicyclo[2,2,2]octane, where the lifetimes are constant and even decrease slightly with increasing *n*. Such increasing *n* retardation of the increase of $\tau(n)$ with increasing *n* in the range $n = 10$–20 may be due to intramolecular mediated cascading via intermediate Rydberg states, where new mediating Rydberg states become effectively coupled with increasing *n* of the doorway state.

We are indebted to R. Bersohn for stimulating discussions and for his incisive comments. We are grateful to M. S. Child, U. Even, E. Grant, Ch. Jungen, H. Lefebvre-Brion, F. Merkt, H. J. Neusser and M. Vrakking for helpful discussions. This research was supported by the German–Israel Binational James Franck Program for Laser–Matter Interaction.

Appendix. Radial integral for high-*n* non-penetrating Rydberg states

Two approximations for the off-diagonal radial integrals of Rydberg orbitals were provided. Mahon *et al.* [45] and Ruscic and Berkowitz [29] have presented off-diagonal matrix elements for r^{-2} and r^{-3} coupling between hydrogenic orbitals based on numerical scaling of the diagonal matrix elements. These matrix elements do not contain the quantum defects, and furthermore they violate the exact 'orthogonality'

relation, equation (28). Gilbert and Child [30] advanced a near-threshold approximation for the dipole coupling, which will be extended for quadrupole and polarizability couplings and utilized herein.

In what follows we shall utilize equation (15) for the dipole ($p = 1$ and $\Delta l = \pm 1$), quadrupole ($p = 2$, $\Delta l; = \pm 2, 0$) and polarizability ($p = 3$, $\Delta l = \pm 2, 0$) interactions. For the case of the dipole interaction ($p = 1$) the radial integral in equation (7) is

$$\langle n, l \left| r^{-2} \right| n', l' \rangle = 2a_0^{-2}(\nu\nu')^{-3/2}(\lambda+\lambda'+1)^{-1}[\Gamma(1+\Delta\lambda)\,\Gamma(1-\Delta\lambda)]^{-1}, \qquad (A\,1)$$

where $\Delta\lambda = \lambda - \lambda'$. The relation $[\Gamma(z)\,\Gamma(1-z)]^{-1} = \pi/\sin(\pi z)$ results in the Gilbert–Child [30] equation

$$\langle n, l \left| r^{-2} \right| n', l' \rangle = 2a_0^{-2}\,\nu^{-3/2}(\nu')^{-3/2}(\lambda+\lambda'+1)^{-1}\frac{\sin(\pi\,\Delta\lambda)}{\pi\Delta\lambda}. \qquad (A\,2)$$

Invoking the selection rules $l' = l \pm 1$ (equation (11)) for dipole coupling, the radial integrals assume the form

$$\langle n, l \left| r^{-2} \right| n', l+1 \rangle = a_0^{-2}\,\nu^{-3/2}(\nu')^{-3/2}(l+1+\Delta^{(+)}\delta_l)^{-1} \otimes \{[1+\Delta\delta_l(1)]\,\Gamma(1+\Delta\delta_l(1))\,\Gamma(-\Delta\delta_l(1))\}^{-1}, \qquad (A\,3)$$

where

$$\Delta\delta_l(1) = \delta(1) = \delta(l) - \delta(l+1), \qquad (A\,4a)$$

$$\Delta^{(+)}\delta_l(1) = \frac{\delta(l)+\delta(l+1)}{2}. \qquad (A\,4b)$$

The radial integral for the quadrupole interaction (equation (8)) is obtained from equation (15) in the form

$$\langle n, l \left| r^{-3} \right| n', l' \rangle = 8a_0^{-3}\,\nu^{-3/2}(\nu')^{-3/2} \otimes [(\lambda+\lambda'+2)(\lambda+\lambda'+1)(\lambda+\lambda')]^{-1}[\Gamma(2+\Delta\lambda)\,\Gamma(2-\Delta\lambda)]^{-1}. \qquad (A\,5)$$

This equation can be transformed to the form

$$\langle n, l \left| r^{-3} \right| n', l' \rangle = 8a_0^{-3}\,\nu^{-3/2}(\nu')^{-3/2} \otimes [(\lambda+\lambda'+2)(\lambda+\lambda'+1)(\lambda+\lambda')]^{-1}[1-(\Delta\lambda)^2]^{-1}\frac{\sin(\pi\Delta\lambda)}{\pi\Delta\lambda}. \qquad (A\,6)$$

The radial integral for the $\Delta l = 2$ quadrupole interaction is

$$\langle n', l \left| r^{-3} \right| n, l+2 \rangle = a_0^{-3}\,\nu^{-3/2}(\nu')^{-3/2} \otimes \{[l+2+\Delta\delta_l^{(+)}(2)]\,[l+\tfrac{3}{2}+\Delta\delta_l^{(+)}(2)]\,[l+1+\Delta\delta_l^{(+)}(2)]\}^{-1} \otimes [\Gamma(4+\Delta\delta_l(2))\,\Gamma(-\Delta\delta_l(2))]^{-1}, \qquad (A\,7)$$

where

$$\Delta\delta_l(2) = \delta(l) - \delta(l+2) \qquad (A\,8a)$$

and

$$\Delta\delta_l^{(+)}(2) = \frac{\delta(l)+\delta(l+2)}{2}. \qquad (A\,8b)$$

The radial integral for the $\Delta l = 0$ quadrupole interaction is

$$\langle n, l \left| r^{-3} \right| n', l \rangle = a_0^{-3}(\nu\nu')^{-3/2}\{[l-\delta(l)+1]\,[l-\delta(l)+\tfrac{1}{2}][l-\delta(l)]\}^{-1}. \qquad (A\,9)$$

The radial integral for the $\Delta l = 0$ quadrupole interaction (equation (A 9)) is

considerably larger than the integral for the $\Delta l = 2$ interaction (equation (A 7)) (i.e. by a numerical factor of about $6/\Delta\delta_f(2)$ for large values of l). This conclusion concurs with the analysis of mediation effects in rotational autoionization [44–46].

The radial integral for the anisotropic polarizability (equation (9)) is given from equation (15) as

$$\begin{aligned}\langle n, l \,|r^{-4}|\, n', l' \rangle = {} & 192 a_0^{-4}\, \nu^{-3/2} (\nu')^{-3/2} \\ & \otimes [(\lambda+\lambda'+3)(\lambda+\lambda'+2)(\lambda+\lambda'+1)(\lambda+\lambda')(\lambda+\lambda'-1)]^{-1} \\ & \otimes [\Gamma(3+\Delta\lambda)\,\Gamma(3-\Delta\lambda)]^{-1}. \end{aligned} \tag{A 10}$$

The radial integral for the $\Delta l = \pm 2$ polarizability interaction is

$$\begin{aligned}\langle n, l \,|r^{-4}|\, n', l+2 \rangle = {} & 192 a_0^{-4}\, \nu^{-3/2} (\nu')^{-3/2} \\ & \otimes \{[2l+5+\Delta l_l^{(+)}(2)]\,[2l+4+\Delta\delta_l^{(+)}(2)] \\ & \otimes [2l+3+\Delta\delta_l^{(+)}(2)]\} \\ & \otimes \{[2l+2+\Delta\delta_l^{(+)}(2)]\,[2l+1+\Delta\delta_l^{(+)}(2)]\}^{-1} \\ & \otimes [\Gamma(5+\Delta\delta_f(2))\,\Gamma(1-\Delta\delta_f(2))]^{-1}, \end{aligned} \tag{A 11}$$

where $\Delta\delta_k(2)$ is given by equation (A 8 *a*) and $\Delta\delta_l^{(+)}$ by equation (A 8 *b*). The radial integral for the $\Delta l = 0$ polarizability interaction is readily obtained from equation (A 10).

References

[1] Reiser, G., Habenicht, W., Müller-Dethlefs, K., and Schlag, E. W., 1988, *Chem. Phys. Lett.*, **152**, 119.
[2] Müller-Dethlefs, K., and Schlag, E. W., 1991, *A. Rev. phys. Chem.*, **42**, 109.
[3] Scherzer, W. G., Selzler, H. L., Schlag, E. W., and Levine, R. D., 1994, *Phys. Rev. Lett.*, **72**, 1435.
[4] Scherzer, W. G., Selzler, H. L., and Schlag, E. W., 1993, *Z. Naturforsch.* a, **48**, 1256.
[5] Alt, C., Scherzer, W. G., Selzle, H. L., and Schlag, E. W., 1995, *Chem. Phys. Lett.*, **240**, 457.
[6] Zhang, X., Smith, J. M., and Knee, J. L., 1993, *J. chem. Phys.*, **99**, 3133.
[7] Even, U., Levine, R. D., and Bersohn, R., 1994, *J. phys. Chem.*, **98**, 3472.
[8] Vrakking, M. J. J., and Lee, Y. T., 1995, *Phys. Rev.* A, **51**, R894.
[9] Vrakking, M. J. J., and Lee, Y. T., 1995, *J. chem. Phys.*, **102**, 8818.
[10] Fischer, I., Villeneuve, D. M., Vrakking, M. J. J., and Stolow, A., 1995, *J. chem. Phys.*, **102**, 5566.
[11] Vrakking, M. J. J., Villeneuve, D. M., and Stolow, A., 1995, *J. chem. Phys.*, **103**, 4538.
[12] Merkt, F., 1994, *J. chem. Phys.*, **100**, 2623.
[13] Even, U., and Mühlpfort, M., 1995, *J. chem. Phys.*, **103**, 4427.
[14] Merkt, F., Mackenzie, S. R., and Softley, T. P., 1995, *J. chem. Phys.*, **103**, 4509.
[15] Bordas, C., Brevet, P. F., Broyer, M., Chevaleyre, J., Labastie, P., and Perrot, J. P., 1988, *Phys. Rev. Lett.* **60**, 917.
[16] Chupka, W. A., 1993, *J. chem. Phys.*, **98**, 4520.
[17] Chupka, W. A., 1993, *J. chem. Phys.*, **99**, 5800.
[18] Bahat, D., Even, U., and Levine, R. D., 1993, *J. chem. Phys.*, **98**, 1744.
[19] Even, U., Ben-Nun, M., and Levine, R. D., 1993, *Chem. Phys. Lett.*, **210**, 416.
[20] Rabani, E., Baranov, L. Ya., Levine, R. D., and Even, U., 1994, *Chem. Phys. Lett.*, **221**, 473.
[21] Rabani, E., Levine, R. D., Mühlpfordt, A., and Even, U., 1995, *J. chem. Phys.*, **102**, 1619.
[22] Merkt, F., and Zare, R. N., 1994, *J. chem. Phys.*, **101**, 3495.
[23] Jortner, J., and Bixon, M., 1995, *J. chem. Phys.*, **102**, 5636.
[24] Bixon, M., and Jortner, J., 1995, *J. phys. Chem.*, **99**, 7466.
[25] Bixon, M., and Jortner, J., 1995, *J. chem. Phys.*, **103**, 4431.

[26] Bixon, M., and Jortner, J., 1996 *J. chem. Phys.* (in press).
[27] Eyler, E. E., and Pipkin, F. M., 1985, *Phys. Rev.* A, **27**, 2469.
[28] Eyler, E. E., 1986, *Phys. Rev.* A, **34**, 2881.
[29] Ruscic, B., and Berkowitz, J., 1990, *J. chem. Phys.*, **93**, 1747.
[30] Gilbert, R. D., and Child, M. S., 1991, *Chem. Phys. Lett.*, **187**, 153.
[31] Lefebvre-Brion, H., and Field, R. W., 1986, *Perturbations in the Spectra of Diatomic Molecules* (Orlando, FL: Academic Press).
[32] Green, C. M., and Jungen, Ch., 1985, *Adv. at. molec. Phys.* **21**, 51.
[33] Fredin, S., Gauyacq, D., Horani, M., Jungen, Ch., Lefevre, G., and Masnou-Seeuws, F., 1987, *Molec. Phys.*, **60**, 825.
[34] Eyler, E. E., and Biernacki, D. T., 1988, *J. chem. Phys.*, **88**, 2851.
[35] Tonkyn, R. G., Wiedmann, R., Grant, E. R., and White, M. G., 1991, *J. Chem. Phys.*, **95**, 7033.
[36] Lee, M. T., Wang, K., McKoy, V., Tonkyn, R. G., Wiedman, R. T., Grant, E. R., and White, M. G., 1992, *J. chem. Phys.*, **96**, 7848.
[37] Bethe, H., and Salpeter, E. E., 1957, *Quantum Mechanics of One- and Two-Electron Atoms* (Berlin: Springer).
[38] Berry, R. S., 1966, *J. chem. Phys.*, **45**, 1228.
[39] Bradsley, N., 1967, *Chem. Phys. Lett.*, **1**, 229.
[40] Russek, A., Patterson, M. R., and Becker, R. L., 1967, *Phys. Rev.*, **167**, 167.
[41] Mulliken, R. S., 1969, *J. Am. chem. Soc.*, **91**, 4615.
[42] Jungen, Ch., and Dill, D., 1980, *J. chem. Phys.*, **73**, 3338.
[43] Herzberg, G., and Jungen, Ch., 1982, *J. molec. Spectrosc.*, **41**, 425.
[44] Bordas, C., Brevet, P., Boyer, M., Chevaleyre, J., and Lebaste, P., 1987, *Europhys. Lett.*, **3**, 789.
[45] Mahon, C. R., Janik, G. R., and Gallagher, T. F., 1990, *Phys. Rev.* A, **41**, 3746.
[46] Merkt, F., Fielding, H. H., and Softley, T. P., 1993, *Chem. Phys. Lett.*, **202**, 153.
[47] Herzberg, G., and Jungen, Ch., 1986, *J. chem. Phys.*, **84**, 1181.
[48] Herzberg, G., and Jungen, Ch., 1982, *J. chem. Phys.*, **77**, 5876.
[49] Gallagher, T., 1994, *Rydberg Atoms* (Cambridge University Press), p. 348.
[50] Buckingham, A. D., 1965, *Discuss. Faraday Soc.*, **40**, 232.
[51] Miescher, E., 1966, *J. molec. Spectrosc.*, **20**, 130.
[52] Miescher, E., 1976, *Can. J. Phys.*, **54**, 2974.
[53] Miescher, E., and Alberti, F., 1976, *J. phys. Chem.*, **5**, 309.
[54] Miescher, E., and Huber, K. P., 1976, *International Reviews of Science, Physical Chemistry* Series 2, Vol. 3. (London: Butterworth).
[55] Killpoar, P. C., Leroi, G. E., Berkowitz, J., and Chupka, W. A., 1973, *J. chem. Phys.*, **58**, 803.
[56] Alberti, F., and Douglas, A. E., 1975, *Can. J. Phys.*, **53**, 1179.
[57] Miescher, E., Lee, Y. T., and Gürtler, P., 1978, *J. chem. Phys.*, **68**, 2753.
[58] Müller-Dethlefs, K., Sander, M., and Schlag, E. W., 1984, *Chem. Phys. Lett.*, **112**, 291.
[59] Müller-Dethlefs, K., Sander, M., and Schlag, E. W., 1984, *Z. Naturforsch.* a, **39**, 1089.
[60] Anekazi, Y., Ebata, T., Mikami, N., and Ito, M., 1985, *Chem. Phys.*, **97**, 153.
[61] Biernacki, D. T., and Colson, S. D., 1988, *J. chem. Phys.*, **88**, 2099.
[62] Nakashima, K., Nakamura, H., Achiba, Y., and Kimura, K., 1989, *J. chem. Phys.*, **91**, 1603.
[63] Gauyacq, D., Roche, A. L., Seaver, M., Consoln, S. D., and Chupka, W. A., 1990, *Molec. Phys.*, **71**, 1311.
[64] Fuji, A., and Norita, N., 1992, *J. chem. Phys.*, **97**, 327.
[65] Fuji, A., and Norita, N., 1993, *J. chem. Phys.*, **98**, 4581.
[66] Fuji, A., and Norita, N., 1995, *J. chem. Phys.*, **103**, 6069.
[67] Pratt, S. T., 1993, *J. chem. Phys.*, **98**, 9241.
[68] Nussenzweig, A., and Eyler, E. E., 1994, *J. chem. Phys.*, **101**, 4617.
[69] Jungen, Ch., 1970, *J. chem. Phys.*, **53**, 4168.
[70] Giusti-Suzor, A., and Jungen, Ch., 1984, *J. chem. Phys.*, **80**, 986.
[71] Raoult, M., 1987, *J. chem. Phys.*, **87**, 4736.

[72] NAKAMURA, K., NAKAMURA, H., ACHIBA, Y., and KIMURA, K., 1989, *J. chem. Phys.*, **91**, 1603.
[73] JUNGEN, CH., and LEFEBVRE-BRION, H., 1970, *Molec. Spectrosc.* **33**, 520.
[74] GRAY, J. A., FERROW, R. L., DURANT, J. L., and THORNE, L. R., 1993, *J. chem. Phys.*, **99**, 4327.
[75] GLENDENING, E. G., FELLER, D., PATTERSON, K. A., and MILLER, R. J., 1995, *J. chem. Phys.*, **103**, 3517.
[76] BILLINGSLEY, F. P., and KRAUS, M., 1974, *J. chem. Phys.*, **60**, 2767.
[77] BRIDGE, N. J., and BUCKINGHAM, A. D., 1966, *Proc. R. Soc.* A, **295**, 334.
[78] WATSON, J. K. G., 1994, *Molec. Phys.*, **81**, 277.
[79] ZON, B. A., 1992, *Soviet Phys. JETP*, **75**, 19.
[80] FEINBERG, G., 1958, *Phys. Rev.*, **112**, 1637.
[81] PASTERNACK, S., and STERNHEIMER, M., 1962, *J. math. Phys.*, **3**, 1280.
[82] ARMSTRONG, L., 1971, *Phys. Rev.* A, **3**, 1546.
[83] BIXON, M., and JORTNER, J., 1996 *J. phys. Chem.* (in press).
[84] AMIRAV, A., HOROVITZ, C., and JORTNER, J., 1988, *J. chem. Phys.*, **88**, 3092.